

# USPEECH: Ultrasound-Enhanced Speech with Minimal Human Effort via Cross-Modal Synthesis

Luca Jiang-Tao Yu <sup>\*†</sup>, Running Zhao <sup>\*†</sup>, Sijie Ji<sup>†</sup>, Edith C.H. Ngai<sup>†</sup>, and Chenshu Wu<sup>†</sup>

<sup>†</sup>The University of Hong Kong

lucayu@connect.hku.hk, rnzhao@connect.hku.hk, sijieji@hku.hk,  
chngai@eee.hku.hk, chenshu@cs.hku.hk

**Project:** <https://aiot-lab.github.io/USpeech/>

## Abstract

Speech enhancement is crucial in human-computer interaction, especially for ubiquitous devices. Ultrasound-based speech enhancement has emerged as an attractive choice because of its superior ubiquity and performance. However, inevitable interference from unexpected and unintended sources during audio-ultrasound data acquisition makes existing solutions rely heavily on human effort for data collection and processing. This leads to significant data scarcity that limits the full potential of ultrasound-based speech enhancement. To address this, we propose USPEECH, a cross-modal ultrasound synthesis framework for speech enhancement with minimal human effort. At its core is a two-stage framework that establishes correspondence between visual and ultrasonic modalities by leveraging audible audio as a bridge. This approach overcomes challenges from the lack of paired video-ultrasound datasets and the inherent heterogeneity between video and ultrasound data. Our framework incorporates contrastive video-audio pre-training to project modalities into a shared semantic space and employs an audio-ultrasound encoder-decoder for ultrasound synthesis. We then present a speech enhancement network that enhances speech in the time-frequency domain and recovers the clean speech waveform via a neural vocoder. Comprehensive experiments show USPEECH achieves remarkable performance using synthetic ultrasound data comparable to physical data, significantly outperforming state-of-the-art ultrasound-based speech enhancement baselines. USPEECH is open-sourced at <https://github.com/aiot-lab/USpeech/>.

## 1 Introduction

Speech is the key enabler for human-computer interaction (HCI) with its potential to create more natural, accessible, and engaging interactions between humans and smart devices, especially for mobile phones that are common devices in lives [18, 54, 94]. Speech-based mobile applications such as virtual assistants [39], smart home control [5, 25], and speech translation software [55, 87] are revolutionizing our daily life. However, speech signals captured in real-world environments are often corrupted by various types of noise and interference, such as background noise, reverberation, and competing speakers, resulting in the well-known cocktail party problem. Unlike the human auditory system, it is challenging for machines to filter out the noise and irrelevant speech to pick up the desired speech command [3]. Consequently, speech enhancement, which aims to improve the quality and intelligibility of desired speech signals, is often considered an essential and critical processing step for many speech-related HCI applications [9, 53, 80].

Decades of efforts have been devoted to audio-only solutions [17, 28, 42, 51, 64, 65, 77, 99]. Recently, with the development of multimodal learning, combining other modalities reflecting vocal information demonstrates additional gains for audio-only solutions, such as video [26], accelerometers [35], millimeter-wave

---

<sup>\*</sup>Equal contribution.

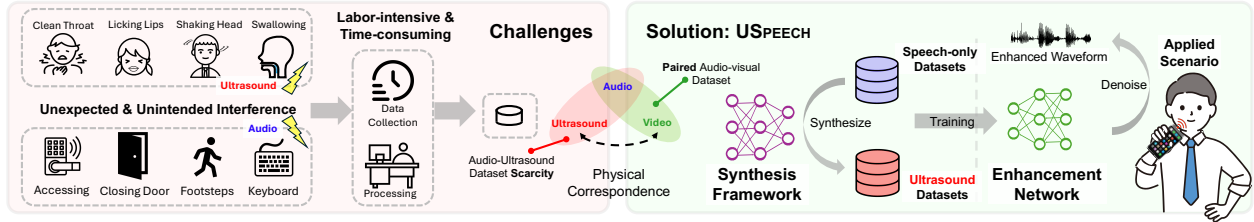


Figure 1: An illustration of challenges in the audio-ultrasound dataset construction and an overview of USPEECH design.

(mmWave) radar [62], magnetic resonance imaging (MRI) and ultrasound tongue imaging (UTI<sup>1</sup>) [76]. At a high level, these secondary modalities capture speech-induced motions at the desired *source* where voice is generated, providing complementary contexts to audio recorded by a microphone at the *destination* where all environmental sounds are mixed. Nonetheless, these modalities suffer from different drawbacks. Videos are privacy-intrusive and susceptible to lighting conditions. MRI, UTI, and mmWave radar rely on specialized equipment unavailable on ubiquitous mobile devices. Accelerometers are ubiquitous, but suffer from low sampling frequency and low sensitivity, preventing them from capturing fine-grained vibrations of speech.

Differently, ultrasound-enhanced speech has emerged as a promising technology recently [14, 78], capitalizing on the relationship between ultrasound and audio to improve the clarity and intelligibility of speech signals. Ultrasound-based solutions leverage acoustic sensing [4, 33] on commodity speakers and microphones without requiring any extra hardware, maintaining superior ubiquity while offering better performance. Specifically, the speaker emits an ultrasound wave that is inaudible to the human ear, while the microphone captures both the audible speech and the reflected ultrasound signal. This signal encodes the information about the speaker’s articulatory motions, which can then be used to further enhance the quality of the speech.

Existing ultrasound-based solutions [14, 78] rely heavily on human efforts for data collection and processing, which is both labor-intensive and time-consuming. This is due to the unavoidable occurrence of unexpected and unintended interferences during the collection of audio-ultrasound data (Fig. 1). Unexpected interference, such as ambient noise from footsteps, closing the door, or even keyboard typing, can significantly degrade the quality of collected human speech. Additionally, unintended human actions like throat clearing, licking lips, *etc.*, can also introduce noise that may overpower the desired ultrasound signal. Interference-affected data can hinder the convergence speed of the network training and even impair the performance [58, 95]. Therefore, once the interference occurs, researchers either need to precisely control the interference factor to re-collect the sample or put considerable effort into processing the data to mitigate the impact. As a consequence, building ultrasound datasets is not only complex but also prohibitively inefficient, creating a notorious data scarcity issue in ultrasound-based speech enhancement.

In this paper, we aim to overcome this problem of data scarcity by building a synthesizer to generate reliable ultrasound data, reducing human efforts. To this end, the video becomes an ideal lever for generating ultrasound, as they both share certain physical correspondence and represent articulatory gesture information, where video reflects the gesture in a visual format and ultrasound unveils that via Doppler shift. However, the lack of paired video-ultrasound datasets poses a significant challenge for synthesizing ultrasound data from videos. Collecting such a dataset also requires extensive human effort. Fortunately, a unique opportunity exists in large-scale paired video-audio datasets that are publicly available, such as YouTube. This motivates us to employ audio as the bridge to connect video and ultrasound. Specifically, we leverage the paired video-audio data with contrastive learning technology to inject the articulatory gestures from videos into audio embeddings, and then use a small set of audio-ultrasound paired data to activate the information. Such a framework maintains the physical correspondence between video and ultrasound while utilizing the inherent consistency between audio and ultrasound to reduce the heterogeneity between video and ultrasound data. Our key insight is that video that captures articulatory gestures visually and ultrasound

<sup>1</sup>UTI is an imaging technique, employs ultrasound via specialized equipment [73], different from the pseudo-ultrasound signals up to 24 kHz emitted by ubiquitous devices, the focus of USPEECH. We will use the terms *pseudo-ultrasound* and *ultrasound* interchangeably in this paper.

that captures these gestures through Doppler shifts share a similar physical correspondence. Both modalities effectively represent articulatory gestures essential for speech enhancement. Based on this, we propose a two-stage ultrasound synthesis framework that utilizes audio signals aligned with video signals in a semantic content space to generate ultrasound signals. In stage one, we employ contrastive video-audio pre-training to project the audio and video into a shared semantic content space. Leveraging the existing large-scale video-audio dataset, contrastive learning enables audio features to inherit the physical motion properties of video features. In stage two, we combine the pre-trained audio encoder with the ultrasound decoder to activate the physical motion information, constructing the connection between audio and ultrasound.

Building on top of the ultrasound synthesis framework, we advance to build an effective speech enhancement network using the generated ultrasound data. We propose a speech enhancement network based on UNet architecture with Transformer layers to fuse the ultrasound and the noisy speech spectrogram and enhance the speech on the Time-Frequency (T-F) domain. Moreover, we apply the neural vocoder [97] to recover the speech waveform from the enhanced spectrogram directly. Note that our enhancement network can be trained using the generated ultrasound data, reducing the human effort for physical data collection.

We present the complete implementation of USPEECH, as shown in Fig. 1, which incorporates the ultrasound synthesis framework in tandem with the speech enhancement network. We prototype USPEECH and evaluate it under various experiments. USPEECH’s speech enhancement network significantly outperforms state-of-the-art ultrasound-based speech enhancement baselines. At the same time, USPEECH, when leveraging a synthetic dataset, can achieve performance comparable to, if not better, that obtained with a manually collected dataset. Furthermore, USPEECH can boost speech enhancement on noisy large-scale speech-only datasets by leveraging the ultrasound data generated from them. USPEECH is open-sourced at <https://github.com/aiot-lab/USpeech/>. Additionally, we provide various real-world examples at <https://aiot-lab.github.io/USpeech/>.

Our core contributions are summarized as follows:

- We propose USPEECH, the first cross-modal ultrasound synthesis framework for speech enhancement with minimal human effort of data collection and processing.
- We design a two-stage ultrasound synthesis framework, including contrastive video-audio pertaining and audio-ultrasound encoder-decoder network, which utilizes audio as a bridge to relate video and ultrasound for ultrasound synthesis. Based on this, we introduce an effective speech enhancement network by fusing UNet and Transformer, which can be trained from synthesis ultrasound data.
- USPEECH is comprehensively evaluated in real-world scenarios under various settings. Experimental results show that the speech enhancement performance of USPEECH outperforms state-of-the-art ultrasound-based speech enhancement baselines, while our performance on synthetic data is on par with that on physically collected data.

## 2 Preliminaries

### 2.1 Articulatory Gestures

Articulatory gestures refer to the actions to enunciate language used in producing phonemes, the fundamental sound units in speech. The articulation process engages many vocal organs, *e.g.*, lips, teeth, jaw, velum, tongue, vocal folds, and larynx, collectively known as articulators [32], as shown in Fig. 2. The gestures are essential for articulation, allowing us to form the distinct sounds that constitute languages. Each gesture involves a specific motion and a combination of vocal organs. The speech operation can be simplified into two procedures [93]: the source produces an initial sound and the vocal tract modulates it. Different articulators are responsible for producing varied phonemes. For instance, the lips can converge to create bilabial sounds (*e.g.*, /p/, /b/, and /m/), while the teeth can serve as passive articulators for sounds such as /f/ and /v/, produced as air is expelled between the bottom lip and upper teeth. Additionally, the jaw’s movement collaborating with the tongue can produce the constants (*e.g.*, /k/ and /g/) and vowels (*e.g.*, /i/, /u/ and /g/).

Articulatory gestures manifest differently depending on sensing modalities. For example, visual articulatory gestures can capture the motion of visible organs [8], *e.g.*, jaws, larynx and lips, and occasionally tongue

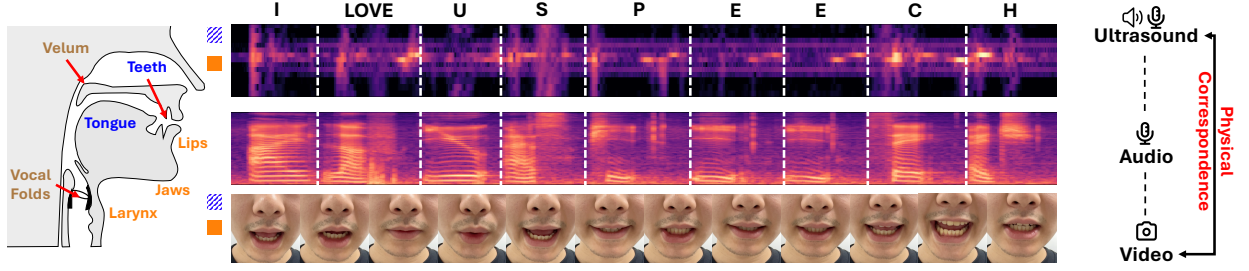


Figure 2: The vocal tract and the physical relationship among three modalities. **Orange** indicates organs *consistently visible*; **Blue** indicates organs that are *occasionally visible*; **Brown** indicates *invisible* organs.

and teeth (shown in Fig. 2). On the other hand, ultrasound articulatory gestures capture more fine-grained vibrations, especially surface vibrations, due to the ultrasound’s high sampling rates [78], underpinning richer contexts for speech enhancement.

## 2.2 Ultrasound Articulatory Sensing

The commodity speaker and microphone in mobile phones transmit the ultrasound wave and receive the reflected ultrasound signal modulated by articulatory gestures for further processing, respectively. The articulatory gestures exhibit velocities ranging from  $-160 \sim 160$  cm/s for bi-directional propagation [83]. According to the Doppler effect, the velocity introduces about  $-94 \sim 94$  Hz Doppler shift within the 20 kHz band. Various sensing waveforms like FMCW [52], OFDM [56], and PN sequences [79, 100] have demonstrated the ability to capture the impulse response but they all suffer from the low sampling rate to capture rapid changes in motion. Ultrasound Continuous Wave (CW) modulated Global System for Mobile Communications (GSM) sequence is applied to calculate the Channel Impulse Response [14], which is constrained by its single-measurement approach that could lead to measurement errors. To address these challenges, particularly the issue of low sampling rates and the need for multiple measurements, we propose to apply the multi-tone CW, treating each tone as one independent measurement. The transmitting signal can be formulated as follows:

$$s(t) = \sum_{i=0}^{N-1} \cos [2\pi(f_0 + i\Delta f) + \phi_i], \quad (1)$$

where the original frequency  $f_0$  is set to 17.25 kHz, the frequency interval  $\Delta f$  is set to 750 Hz and the number of tones  $N$  is set to 8. We set the sampling rate as 48 kHz. The received signal can be expressed as:

$$r(t) = \sum_{i=0}^{N-1} \cos \left[ 2\pi \left( 1 + \frac{\Delta v}{c} \right) (f_0 + i\Delta f) + \phi_i + \Delta \phi_i \right], \quad (2)$$

where  $\Delta v$  and  $c$  indicate the velocity of articulatory gestures and sound speed. To obtain the Doppler shift related to articulatory gestures, we then perform STFT and signal processing.

## 3 Challenges and Opportunities

### 3.1 Difficulties in Ultrasound Dataset Construction

Building a clean audio-ultrasound dataset faces lots of difficulties. As discussed in Section 1, existing works suffer from intensive human efforts for data collection and processing. As illustrated in Fig. 3, both audio and ultrasound spectrograms suffer from sensitivity to unexpected interference from the environments. The audio is susceptible to ambient noise, such as accessing the room, closing the door, human footsteps, keyboard typing, *etc.*. Similarly, as the ultrasound captures fine-grained human movements, it is susceptible to unintended human-related actions, even subtle motions that often go unnoticed, like cleaning the throat,

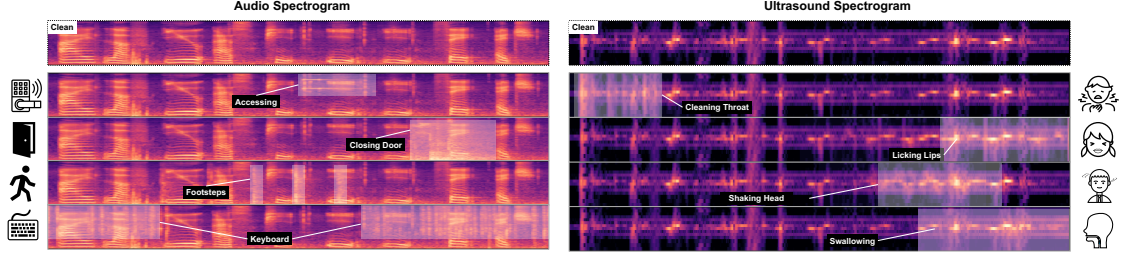


Figure 3: Different unexpected and unintended interference on the audio and ultrasound spectrograms when collecting the audio-ultrasound dataset.

licking lips, shaking the head, swallowing, *etc.*. In some instances, the noise can have higher energy than the desired signal. As a result, the data affected by the above interference can hinder the convergence speed of the network training and even impair the performance. Consequently, collecting a high-quality clean dataset requires a quiet room, which imposes significant constraints. Volunteers are also required to deliberately control their actions over extended periods, which is impractical in real collection scenarios. Otherwise, substantial human effort for signal processing is needed to process the dataset before use. Therefore, once this occurs, lots of effort is required to process the interference, or interference factors need to be precisely controlled for re-collection. Besides, the intelligibility and the quality of enhanced spectrogram and waveform are susceptible to the quality of a clean dataset. Additionally, publicity of the collected dataset is limited due to the privacy concerns of the volunteers. To address these issues, we propose an ultrasound synthesis framework to generate ultrasound datasets from audio datasets, while only requiring a small-scale dataset for training. By minimizing the size of the dataset we need to collect, we mitigate the rate of unexpected interference, thereby minimizing the amount of human effort.

### 3.2 Speech in Video, Audio, and Ultrasound

As mentioned above, both video and ultrasound modalities are capable of capturing articulatory gestures during speech production, with Fig. 2 illustrating the physical relationships between video and ultrasound. Taking the phoneme /v/ from the word "love" as an example, we observe that its production involves high-frequency, fine-grained vibrations of the larynx coupled with lip closure. The specific movements correspond to the second interval on ultrasound recordings and are visually discernible in the second and third frames of the video. The observation validates the physical correspondence between video and ultrasound. However, paired video-ultrasound datasets with speech labels are missing, and more importantly, very costly to build. The different representation forms of video and ultrasound also pose a challenge for the modality transformation. For the same example, it can be seen in Fig. 2 that the audio spectrogram captures the distinct sound of the /v/ phoneme at a similar position. This reveals that audio shares similar representation forms of time series with ultrasound. This promises an opportunity to leverage audio as the bridge to relate video and ultrasound, thereby generating massive audio-ultrasound data from large-scale audio-video data, which are widely available online. By doing so, we can overcome all the drawbacks shown in Fig. 1.

## 4 USPEECH Overview

In this section, we elaborate on the overall structure of USPEECH, which contains an ultrasound synthesis framework (§5.1) and a speech enhancement network (§5.2).

**Ultrasound Synthesis Framework:** The synthesis framework contains two stages (see Fig. 4):

1) *Contrastive Video-Audio Pre-training:* The contrastive video-audio pertaining projects the audio and video into a shared semantic content space. It utilizes open-source video-audio datasets containing the visual articulatory gestures to pre-train the video encoder and audio encoder via contrastive learning. This learning process injects the articulatory gestures from videos into audio embeddings, enabling the audio encoder to inherit the physical motion properties.



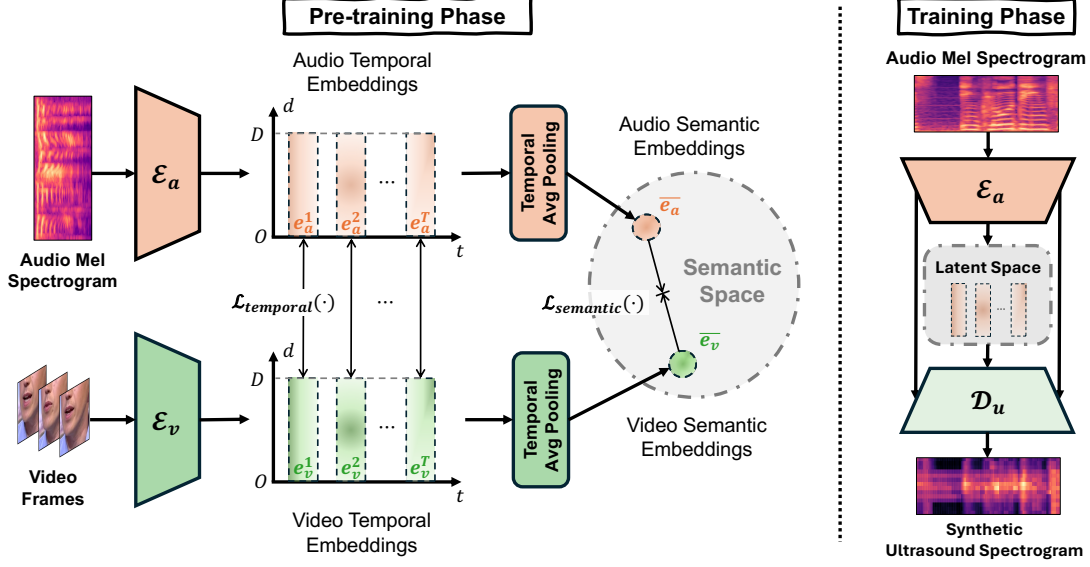


Figure 4: An overview of ultrasound synthesis framework. It includes the contrastive video-audio pre-training phase (left) for projecting video and audio into a shared semantic content space, and the training phase (right) about the audio-ultrasound encoder-decoder network for constructing the connection between audio and ultrasound.

2) *Audio-Ultrasound Encoder-Decoder Network*: After contrastive video-audio pre-training, the pre-trained audio encoder is capable of encoding the audio into embeddings containing physical properties of articulatory gestures. Subsequently, to adapt the information from audio to ultrasound, we design a UNet-based network with the pre-trained audio encoder and the ultrasound decoder to transform the above embeddings into the ultrasound Doppler shift spectrogram.

**Speech Enhancement Network**: The enhancement network contains two phases (see Fig. 5):

1) *Mel Spectrogram Enhancement*: The first phase is a UNet network that enhances the Mel spectrogram by taking ultrasound and noisy speech as input. The encoded embeddings of ultrasound and noisy speech are fused by the Transformer layers and then, the fused embeddings are decoded into Mel spectrogram of enhanced speech.

2) *Waveform Recovery*: In the second phase, we leverage a neural vocoder to recover the high-quality enhanced speech waveform from the enhanced Mel spectrogram.

## 5 USPEECH Design

In this section, we commence by detailing the synthesis process of ultrasound. Following this, we detail the design of the speech enhancement network.

### 5.1 Ultrasound Synthesis

#### 5.1.1 Contrastive Video-Audio Pre-training

As previously outlined, our approach harnesses contrastive learning [69] to align the video-audio representation both temporally and semantically. We utilize the LRW [10] video-audio dataset to pre-train the model. Considering that we are not interested in facial identification, we crop a  $128 \times 128$  region centered around the mouth to focus on visual articulatory gestures, as illustrated in Fig. 2. To better align the temporal audio embeddings, we replicate the last frame, resulting in all input videos having the shape  $x_v \in \mathbb{R}^{30 \times 3 \times 128 \times 128}$ . For the audio data, we resample them into 16 kHz and transform them using a Mel filter with an FFT size of 1024, 128 Mel bands, and a hop size of 160. Consequently, the audio data are represented as  $x_a \in \mathbb{R}^{122 \times 128}$ ,

where 122 corresponds to the time bins of the Mel spectrogram, and 128 represents the Mel frequency bins. We subsequently use the decibel scale of the Mel spectrogram. Overall, in video-audio representation alignment, we pre-train the audio encode  $\mathcal{E}_a$  and video encoder  $\mathcal{E}_v$  using the data pair  $(x_v, x_a)$ .

To increase the representation ability of audio embeddings, we adapt the audio encoder architecture from [45], originally pre-trained on the Audioset dataset [31], by modifying the output layers to adjust the embedding representation with the Mel-scale spectrogram of speech. The model comprises six convolutional blocks, and each block includes a sequence of two 2D convolutional layers, followed by two 2D convolutional layers, a batch normalization layer, a ReLU function, and an average pooling layer. After the convolutional blocks, the feature map is directed through average and max pooling processes independently, with the results subsequently added to extract latent information. By applying both pooling operations and then adding their results, the network is able to extract a richer combination of both strong and subtle features, ensuring that none of the important information is lost in the process. The additional feature map then undergoes two fully connected layers with the output dimensions of 2048 and 512, respectively, which can further improve the representation ability. Except for the final layer, each fully connected layer is equipped with a linear layer followed by a ReLU function. Ultimately, the audio encoder will output the speech temporal embeddings which are time-aligned with video embeddings across temporal segments.

To design the video encoder component, we draw inspiration from the SlowOnly backbone of the SlowFast architecture, introduced by [24], which has been pre-trained on the Kinetics-400 dataset [44]. In our adaptation, we modify the input layer to accommodate the specific shape of video inputs. Additionally, we introduce fully connected layers to further refine the extracted features. These layers serve an important role in transforming the feature map into a compact and meaningful representation, projecting it to the desired 512-dimensional space. This step is crucial for effectively capturing and encoding the visual articulatory gestures, ensuring the model can interpret the temporal and spatial patterns critical for the task. By adding these layers, the model learns a more effective representation, enhancing its ability to generalize across different video inputs.

Denote the output shape of audio and video encoder as  $e_a \in \mathbb{R}^{T \times D}$  and  $e_v \in \mathbb{R}^{T \times D}$ , where  $T$  and  $D$  are the temporal segments and feature dimension, respectively, paired as set  $\mathcal{T} = \{e_a, e_v\}$ . Then we apply the temporal average pooling for each temporal embedding on the temporal segments to get the corresponding semantic embedding  $\bar{e}_a \in \mathbb{R}^D$  and  $\bar{e}_v \in \mathbb{R}^D$ , paired as set  $\mathcal{S} = \{\bar{e}_a, \bar{e}_v\}$ . To align the representations temporally and semantically in contrastive learning [50], we propose temporal loss  $\mathcal{L}_{temporal}(\cdot)$  computed on  $\mathcal{T}$  and semantic loss  $\mathcal{L}_{semantic}(\cdot)$  computed on  $\mathcal{S}$  based on InfoNCE loss [60]. The temporal loss aims to maximize the intra-segment while minimizing the inter-segment similarity within the same video. Similarly, semantic loss seeks to enhance the similarity between identical video-audio embeddings and reduce it across disparate embeddings. The per-sample pair loss can be formulated as:

$$\mathcal{L}_{temporal}^{(i,j)} = -\frac{1}{2} \log \frac{\exp(\text{sim}(e_a^i, e_v^j)/\tau)}{\sum_{k=1}^{n_t} \exp(\text{sim}(e_a^i, e_v^k)/\tau)} - \frac{1}{2} \log \frac{\exp(\text{sim}(e_a^j, e_v^i)/\tau)}{\sum_{k=1}^{n_t} \exp(\text{sim}(e_a^k, e_v^j)/\tau)}, \quad (3)$$

$$\mathcal{L}_{semantic}^{(i,j)} = -\frac{1}{2} \log \frac{\exp(\text{sim}(\bar{e}_a^i, \bar{e}_v^j)/\tau)}{\sum_{k=1}^{n_s} \exp(\text{sim}(\bar{e}_a^i, \bar{e}_v^k)/\tau)} - \frac{1}{2} \log \frac{\exp(\text{sim}(\bar{e}_a^j, \bar{e}_v^i)/\tau)}{\sum_{k=1}^{n_s} \exp(\text{sim}(\bar{e}_a^k, \bar{e}_v^j)/\tau)}, \quad (4)$$

where  $\text{sim}(\cdot)$  denotes the cosine similarity function,  $n_t$  and  $n_s$  indicate the number of temporal segments within one video and the number of different video-audio embeddings, and  $\tau$  is the scaled temperature parameter (default 0.07). Thus, the overall contrastive learning loss is formulated as a weighted sum of the temporal and semantic losses, with  $\lambda$  (default 0.5) serving as the weighting coefficient. This approach balances the influence of temporal alignment and semantic similarity, formulated as:

$$\mathcal{L}_{contrastive} = \lambda \mathcal{L}_{temporal} + (1 - \lambda) \mathcal{L}_{semantic}. \quad (5)$$

### 5.1.2 Audio-Ultrasound Encoder-Decoder Network.

After employing contrastive learning to align video-audio representations temporally and semantically, the audio encoder becomes capable of transforming an audio Mel spectrogram into embeddings that are rich in visual articulatory information. This capability suggests that the pre-trained audio encoder has effectively learned to represent the visible articulatory gestures associated with the audio. Consequently, we directly

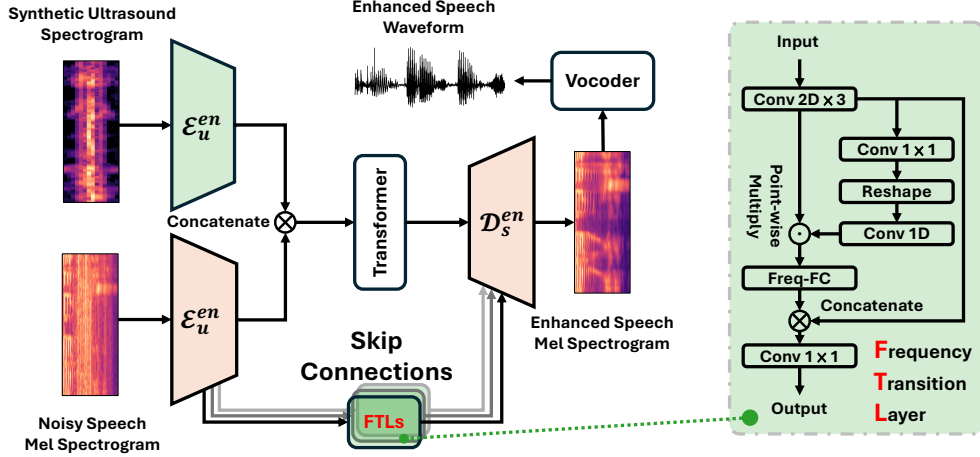


Figure 5: An overview of speech enhancement network, including Mel spectrogram enhancement and waveform recovery (middle). The architecture of the Frequency Transition Layer (FTL) is shown on the right.

deploy the pre-trained audio encoder in synthesizing the ultrasound Doppler shift spectrogram. We utilize the collected small-scale dataset for ultrasound synthesis framework training. Because the collected audio data consist of low-frequency speech and high-frequency ultrasound articulatory signals, we apply an 8th-order elliptic lowpass filter with a cutoff frequency of 8 kHz and a highpass filter with a cutoff frequency of 16 kHz to separate the speech and ultrasound components, respectively. For speech, after filtering, we downsample the speech from 48 kHz to 16 kHz and apply the same processing to obtain the Mel spectrogram, resulting in a tensor of shape  $x_s \in \mathbb{R}^{T \times 128}$ . For ultrasound, to synchronize with speech, we compute the STFT spectrogram with an FFT size of 8192, a window size of 8160, and a hop size of 480, resulting in approximately 5.86 Hz frequency resolution. To mitigate the static background and direct reflections in the ultrasound spectrogram, we drop the central frequency bin along with its adjacent 2 bins corresponding to the Doppler shifts  $\pm 5.86, 0$  Hz. We keep the other  $7 \times 2$  bins around the central frequency bins of each tone, corresponding to the Doppler shifts in the ranges  $[-5.86 \times 8, -5.86)$  Hz and  $(5.86, 5.86 \times 8]$  Hz. As mentioned in §2.2, we regard the Doppler shift of every single tone as an independent measurement; thus, we calculate the mean of all channels, resulting in a tensor of shape  $x_u^T \in \mathbb{R}^{T \times 14}$ . Overall, in the ultrasound decoder stage, we train the ultrasound decoder  $\mathcal{D}_u$  with the speech encoder  $\mathcal{E}_a$  from the video-audio representation alignment stage using the data pair  $(x_s, x_u)$ .

To fully capture and utilize the rich details in the original features, we integrate a skip connection inspired by the UNet architecture [71], and we concatenate the feature maps of the audio encoder layers with the homologous ultrasound decoder layers. The ultrasound decoder is generally a transposed architecture of the encoder comprising six transposed convolutional layers and a projector. Each transposed convolutional layer is equipped with a transposed convolutional layer and one convolutional block with the same architecture as the audio encoder. To tailor the shape of the feature map, we add a projector as the output layer which is a transposed convolutional layer with the kernel size  $2 \times 1$ , stride size  $2 \times 1$ , padding of 25, and a dilation factor of 1.

Denote the synthesized ultrasound Doppler shift spectrogram as  $d_{syn} \in \mathbb{R}^{T \times F}$ , where  $T$  and  $F$  are the temporal segments and frequency bins, respectively. We apply Mean Square Error (MSE) not only to the Doppler shift spectrogram  $d_{syn}$  but also to the time differential spectrogram  $\Delta d_{syn}$ . This dual application of MSE allows the model to capture not just the static features of the spectrogram but also the dynamic changes over time, thereby enriching the model’s learning with temporal details. The overall supervised learning error is formulated as the  $\alpha$ -weighted (default 0.5) MSE error:

$$\mathcal{L}_{supervised} = \alpha \text{MSE}(d_{syn}, d_{gt}) + (1 - \alpha) \text{MSE}(\Delta d_{syn}, \Delta d_{gt}). \quad (6)$$



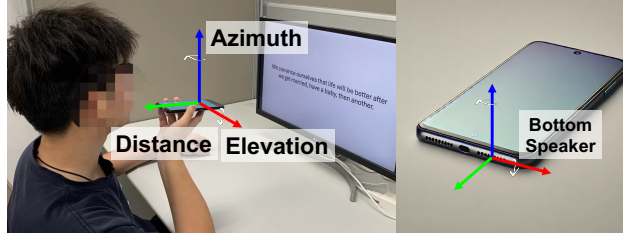


Figure 6: Data collection. Three axes define the device’s coordinate system. The axis depicted in **Green** denotes the distance to the mouth. Rotations about the **Red** axis represent elevation adjustments, and rotations around the **Blue** axis correspond to changes in azimuth.

## 5.2 Speech Enhancement

### 5.2.1 Mel Spectrogram Enhancement

Based on the UNet architecture, we have developed a network for enhancing the Mel spectrogram, as illustrated in Fig. 5. Recognizing the critical role of harmonic correlation across the frequency axis in augmenting the quality of the T-F spectrogram [88], our design incorporates both a UNet-based backbone for contextual temporal information capture and Frequency Transition Layers (FTL) [102]. The FTLs are strategically positioned between each downsampling convolutional layer to enhance harmonic information capture. The FTL consists of three stacked convolutional layers, a fully connected layer used as a transformation matrix, and a  $1 \times 1$  convolutional layer as the output, shown in Fig. 5. Each convolutional layer is comprised of a 2D convolutional layer, followed by batch normalization and a ReLU activation function. Parallel to the speech encoder branch, the ultrasound branch mirrors these settings without FTLs. A key feature of our design is the integration of the Vision Transformer [15, 86] at the bottleneck. This introduces an attention mechanism to the temporal segments of the feature map, leveraging the Transformer’s capabilities pre-trained on ImageNet [13]. The enhancement of the Mel spectrogram is further refined by applying MSE loss.

### 5.2.2 Waveform Recovery

After enhancing the T-F domain spectrogram, we employ a neural vocoder, specifically the Parallel WaveGAN [97], to reconstruct the waveform from the enhanced Mel spectrogram. The phase information plays a pivotal role in accurately recovering waveform from T-F domain spectrograms [63]. However, converting audio signals into Mel spectrograms inherently results in the loss of phase information, which is crucial for reconstructing high-quality natural-sounding waveforms. To overcome this challenge, we employ a neural vocoder that includes both a generator and a discriminator. The generator synthesizes the audio waveform directly from the Mel spectrogram by learning the mapping between the spectrogram and time-domain waveform, while the discriminator helps ensure the generated waveforms sound realistic by distinguishing between real and generated audio. By leveraging adversarial training, the neural vocoder learns not only to reconstruct amplitude but also implicitly recovers the missing phase information. This allows for more accurate and perceptually natural waveform generation, compensating for the phase loss that occurs during the spectrogram conversion process. The vocoder undergoes training through the joint optimization of a multi-resolution spectrogram loss and an adversarial loss [97]. This dual loss approach significantly enhances the model’s ability to replicate the time-frequency distribution characteristic of realistic speech waveforms.

## 6 Experimental Setup

### 6.1 Data Collection

Due to the lossy M4A compression method used by the recorded in standard smartphones, which is not capable of capturing the ultrasound band, we develop an Android application to gather an audio-ultrasound dataset using the OPPO Reno2 Z. Given that a typical smartphone’s earpiece power (about  $5 \mu\text{W}$ ) is too low for sensing purposes, we instead utilized the more powerful bottom-mounted speaker (1 W) along with the

microphone for transmitting and receiving signals. This setup enables us to record the synchrony between ultrasound articulatory and speech accurately. The data collection setup is illustrated in Fig. 6.

We recruit 7 volunteers (2 females and 5 males) to participate in the data collection by reading the selected materials, aiming to construct an audio-ultrasound dataset in an environment with about 50 dB of ambient noise. The experimental setting is regardless of the azimuth and elevation but within the reasonable range from 5 to 10 centimeters between the mouth and the bottom microphone with no rotation of the device. The reading materials comprised a mix of articles, news, and reading materials, outlined in the Appendix Tab. A1. All volunteers read these materials in the same order and the volume of the dataset varies from 70 to 83 dB. Overall, we collected 2.4 hours of audio-ultrasound data for the ultrasound synthesis framework (§6.2.2) and 0.6 hours of audio-ultrasound data for the speech enhancement network (§6.2.3), which are different materials to prevent data leakage and overlaps.

## 6.2 Data Preparation

### 6.2.1 Ultrasound Synthesis Pre-training Dataset

The LRW dataset [10] is the public video-audio dataset that is utilized in the contrastive video-audio pre-training phase (§5.1.1), which comprises approximately 1,000 utterances of 500 distinct words, each with a fixed duration of 1.22 seconds audio and 29 video frames.

### 6.2.2 Ultrasound Synthesis Dataset

We use the collected 2.4-hour audio-ultrasound dataset as the ultrasound synthesis dataset. We split the dataset as training and testing subsets by 4:1, where 1.92 hours to train the audio-ultrasound encoder-decoder network (§5.1.2) and 0.48 hours to test. The dataset does not overlap with all datasets utilized in the training speech enhancement network.

### 6.2.3 Speech Enhancement (SE) Dataset

To assess the enhancement performance of USPEECH, we employ multiple datasets. First, we gather the physical SE dataset to train the speech enhancement network and evaluate the effectiveness of the proposed USPEECH. Second, we utilize an audio-ultrasound network, trained on the ultrasound synthesis dataset, to generate synthetic ultrasound spectrograms from the physical SE dataset, thereby creating the synthetic SE dataset. Finally, we apply the same procedure to large-scale speech-only datasets to generate corresponding ultrasound spectrograms, constructing large-scale synthetic SE datasets.

- **Physical SE Dataset:** We use the collected 0.6-hour audio-ultrasound dataset as the physical SE dataset, where 80% (0.48 hours) to train the speech enhancement network (§6.2.3) and 20% (0.12 hours) to test. We refer to this dataset as "physical" or "phy." in experimental evaluation because it utilizes real-world collected ultrasound spectrograms. The dataset does not overlap with the ultrasound synthesis dataset to prevent data leakage. To adapt the input of other baselines, we also make the complex physical SE dataset, with the same contents while keeping the imaginary part of spectrograms.
- **Synthetic SE Dataset:** Leveraging the ultrasound synthesis framework trained on the ultrasound synthesis dataset, we generate the synthetic SE dataset from the physical SE dataset, where the collected audio Mel spectrograms serve as input and the corresponding ultrasound spectrograms are generated as output. We then pair the audio Mel spectrograms with the synthetic ultrasound spectrograms to form the synthetic SE dataset. This dataset is subsequently split into training and testing sets, maintaining the same proportion as in the physical SE dataset.
- **Large-scale Synthetic SE Datasets:** We employ three distinctive, public, large-scale speech-only datasets for ultrasound generation to evaluate the generalizability of the ultrasound synthesis framework in §7.2. Similar to the synthetic SE dataset, we use the trained synthesis model to generate ultrasound spectrograms from these speech-only datasets, and pair the audio and ultrasound to construct the large-scale synthetic SE datasets. The overview of these large-scale speech-only datasets is as follows:

- **LJSpeech** [41] (24 hours) consists of 13.1k short audio clips from a single female speaker reading passages from 7 non-fiction books. This dataset provides sufficient scale but lacks speaker diversity.
- **TIMIT** [30] (5.8 hours) addresses this limitation by including recordings from 630 speakers (approximately 70% male and 30% female) with diverse features such as gender, dialect, and age. While it offers high speaker diversity, it has a smaller scale compared to LJSpeech.
- **VCTK** [96] (44 hours) contains speech data from 110 speakers with multiple accents, each reading 400 sentences from news articles and other reading materials. This dataset provides both sufficient scale and speaker diversity.

For speech enhancement network training, we generate the **Noisy SE Dataset** by mixing the clean speech we collected with the noise source dataset Nonspeech7k [70]. The dataset contains *human’s nonspeech*, *e.g.* screaming, crying, coughing, from freesound.org, YouTube, and Aigei, rather than the ambient noise, which has a more similar distribution with the speech. Each clean speech sample is mixed with 20 different noises in collected physical and synthetic SE datasets and 1 noise in large-scale synthetic SE datasets, and the mixing process is with the specific SNRs randomly chosen from  $\{-10, -5, 0, 5, 10, 15\}$  dB.

### 6.3 Baselines

To illustrate the effectiveness of the proposed USPEECH, we select three baselines for comparison. We choose ultrasound-based speech enhancement methodologies, *i.e.*, Ultraspeech [14] and UltraSE [78]. We utilize the complex physical SE dataset (*i.e.*, including the imaginary part of spectrograms) to evaluate all baselines because the inputs are complex spectrograms. Specifically, we adjust the input layer of Ultraspeech to adapt the input shape and only implement the enhancement component. In addition, we choose a speech-only baseline PHASEN [99] to show the effectiveness of the involvement of ultrasound. The overview of the model design is as follows:

- **Ultraspeech** [14]: The model utilizes a two-branch neural network for speech enhancement, combining ultrasound and speech signals. It uses a complex ratio mask to estimate noisy speech’s magnitude and phase components. The interaction module allows information exchange between ultrasound and speech branches, improving noise discrimination.
- **UltraSE** [78]: The model borrows a multi-modal design for single-channel speech enhancement using ultrasound and speech signals. It employs a two-stream architecture to process speech and ultrasound separately, followed by a self-attention fusion mechanism to integrate the features. The model also uses a cGAN-based cross-modal training model to enhance the noisy speech spectrograms.
- **PHASEN** [99]: The model features two parallel streams for amplitude and phase prediction. The amplitude stream includes frequency transformation blocks to capture global frequency correlations, while the phase stream benefits from information exchange between the streams, allowing the model to enhance both amplitude and phase.

### 6.4 Training Details

We provide training details on our model for reproduction. For both stages, we employ the automatic mixed-precision mode and AdamW [49] optimizer except the vocoder with RAdam [47] optimizer. The hyperparameters  $\lambda$  and  $\alpha$  of weighted loss are both set to 0.5.

#### 6.4.1 Ultrasound Synthesis Framework

In contrastive video-audio pre-training, we apply contrastive learning to train the model with 4 NVIDIA 4090 GPUs for 10 hours to converge with a batch size of 256. We utilize the cosine decay warmup scheduler to adjust the learning rate during the training phase with the initial learning rate  $8 \times 10^{-4}$  and warmup steps 600. In the audio-ultrasound encoder-decoder network, we apply supervised learning to train the model with 2 NVIDIA 4090 GPUs for 2 hours with a batch size of 128. We utilize the cosine decay warmup scheduler as well with the starting learning rate  $1 \times 10^{-3}$  and warmup steps 200.

### 6.4.2 Speech Enhancement Network

In Mel spectrogram enhancement, we apply supervised learning to train the enhancement model with 4 NVIDIA 4090 GPUs for 4 hours with a batch size of 128. We apply the StepLR scheduler to reduce the learning rate by half for each 6.3k steps. In waveform recovery, we separately train it from Mel spectrogram enhancement with 4 NVIDIA 3090 GPUs for 25 hours with a minibatch size of 8 and each sample is 1.0 second. The initial learning rate is set to  $1 \times 10^{-4}$  and  $5 \times 10^{-5}$  for the generator and discriminator, respectively. We utilize the StepLR scheduler to reduce the learning rate by half for each 200k steps. The model contains approximately 90M trainable parameters.

## 6.5 Evaluation Metrics

We use three quantitative metrics (PESQ, STOI, and LSD) and one qualitative metric (MOS) to evaluate the quality of enhanced speech.

**PESQ:** Perceptual Evaluation of Speech Quality [40] is an objective standard for evaluating the quality of speech standardized by ITU-T P.862. PESQ returns a score from -0.5 to 4.5, with higher scores indicating better quality.

**STOI:** Short-Time Objective Intelligibility [81] is an objective metric used to assess the intelligibility of the speech signals which predicts how understandable speech is in various conditions, particularly when the speech is affected by noise and distortion. STOI returns a score from 0 to 1, with higher scores meaning better quality.

**LSD:** Log-Spectral Distance [68] is used to quantify the difference or distortion between two audio signals in the frequency domain, shown in decibels scale. LSD score is better if lower.

**MOS:** Mean Opinion Score [72] is a subjective measurement that is used to evaluate the quality of human-computer interactions. In a typical MOS test, a group of human subjects is asked to rate the quality of media samples on a scale, usually ranging from 1 to 5 (the higher the better quality), shown in the Appendix Tab. B1. We recruit 10 volunteers to conduct a qualitative evaluation of the enhanced speech using MOS. In experiments, we first play the clean speech, then the noisy and its corresponding enhanced speech without knowing whether the enhanced speech from USPEECH. Each volunteer will be assigned 100 samples (20 for each method) randomly chosen from different SNRs. The final results will be average for all volunteers.

## 7 Experimental Evaluation

In this section, we first begin by showcasing the overall performance of USPEECH and other baselines in §7.1, including quantitative and qualitative evaluation. Second, we conduct experiments on ultrasonic large-scale dataset synthesis to further evaluate the effectiveness and generalizability of the synthesis framework in §7.2. Third, we conduct the evaluation on temporal variability to demonstrate the robustness of USPEECH in non-fixed length input in §7.3. Fourth, to better understand the relationship between performance and data scale, we conduct comprehensive experiments in §7.4. After that, we evaluate the stability of enhancement networks on different noise interference in §7.5. Then, we also evaluate unseen user performance in §7.6 and ablation study in §7.7. Last, we conduct a very comprehensive evaluation of the impact of different factors (*e.g.*, distance, azimuth, elevation, device type, *etc.*) in §7.8.

### 7.1 Overall Performance

#### 7.1.1 Visualization Analysis

As shown in Figure 7, the synthetic ultrasound spectrogram visually exhibits a striking similarity to the corresponding physical ultrasound spectrogram in the first column. Additionally, we provide a quantitative evaluation of the synthesis fidelity across samples. We use the Structural Similarity Index Measure (SSIM) [90], a widely recognized metric that assesses similarity by analyzing the means and covariances of two samples, to evaluate the similarity between the synthetic and real ultrasound spectrograms. Each column shows the corresponding samples, with the SSIM value of the synthetic ultrasound spectrogram displayed at the bottom left. For example, the first spectrogram shows a fidelity of 0.86 compared with the physical spectrogram. We can clearly see that the first peak is generated at the correct temporal interval, well aligned

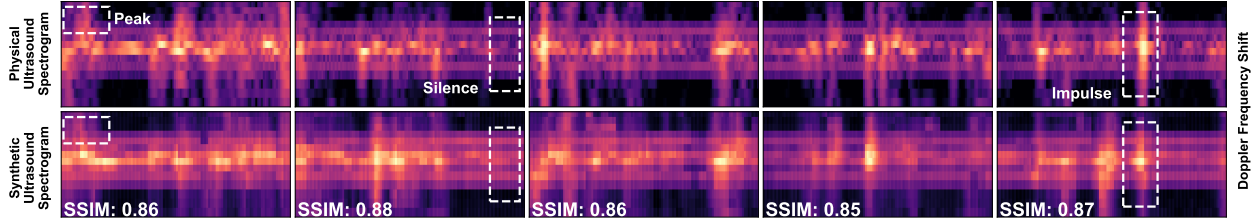


Figure 7: Visualization of the physical *v.s.* USPEECH synthetic ultrasound spectrograms. USPEECH is capable of synthesizing high-quality ultrasound spectrograms, particularly when integrating video information. We calculate the single-spectrogram Structural Similarity Index Measure (**SSIM**) between the physical and USPEECH synthetic ultrasound spectrograms per sample, providing a quantitative measure of synthesis fidelity.

Table 1: Quantitative and qualitative evaluation results. The  $\Delta$  metrics show the improvement or reduction compared with the Noisy SE Dataset. USPEECH w/ syn. or phy. means the speech enhancement network of USPEECH is trained and evaluated on the synthetic or physical SE dataset.

| Method                 | PESQ $\uparrow$ | $\Delta$ PESQ $\uparrow$ | STOI $\uparrow$ | $\Delta$ STOI $\uparrow$ | LSD $\downarrow$ | $\Delta$ LSD $\downarrow$ | MOS $\uparrow$ |
|------------------------|-----------------|--------------------------|-----------------|--------------------------|------------------|---------------------------|----------------|
| Noisy SE Dataset       | 2.33            | -                        | 0.77            | -                        | 1.16             | -                         | -              |
| <b>USPEECH w/ syn.</b> | <b>3.01</b>     | <b>+29.2%</b>            | <b>0.85</b>     | <b>+10.4%</b>            | <b>0.83</b>      | <b>-28.4%</b>             | <b>4.45</b>    |
| <b>USPEECH w/ phy.</b> | <u>2.90</u>     | <u>+24.5%</u>            | <u>0.84</u>     | <u>+9.1%</u>             | <u>0.85</u>      | <u>-26.7%</u>             | <u>4.43</u>    |
| Ultraspeech [14]       | 1.69            | -27.5%                   | 0.57            | -26.0%                   | 2.29             | +97.4%                    | 2.13           |
| UltraSE [78]           | 2.11            | +9.4%                    | 0.77            | 0.0%                     | 1.40             | +20.7%                    | 2.80           |
| PHASEN [99]            | 2.82            | +21.0%                   | <u>0.84</u>     | <u>+9.1%</u>             | 1.12             | -3.4%                     | 3.78           |

with the physical one. In the second sample, the synthesis model accurately generates the silence at the correct time interval. In the last sample, we demonstrate that the model can also generate the impulse of the ultrasound spectrogram. In a nutshell, the synthesis model is capable of generating high-quality ultrasound spectrograms even in different patterns, *e.g.*, peak, silence, impulse, *etc.*.

### 7.1.2 Quantitative Evaluation

We first demonstrate the capability of the speech enhancement network by comparing it with other baselines, and based on this fact, we further validate the effectiveness of the ultrasound synthesis framework.

As illustrated in Tab. 1, we elaborate on the results of USPEECH compared with others. Compared with other baselines trained on the physical SE dataset, USPEECH w/ phy. outperforms in all four metrics, with the PESQ gain of 24.5%, STOI gain of 9.1%, and LSD drop from 1.16 of the noisy dataset to 0.85. The results indicate that the proposed enhancement network is capable of improving quality and intelligibility. While both ultrasound-based speech enhancement Ultraspeech [14] and UltraSE [78] fail to enhance our noisy SE dataset with human-related nonspeech noise. For Ultraspeech, they only utilize the other noise dataset [37] that only contains the ambient noise *e.g.*, musical instruments and machines (*i.e.*, no human’s nonspeech). We observe that Ultraspeech will also increase human-related noise as well, indicating they might not perform as expected when enhancing the human-related noise source [70] we utilized. For UltraSE, they design a complex model with the parameters  $\sim 286$  M, which is too complex for speech enhancement. They do not release code or adversarial hyperparameters, so we implement the neural network and set the proper margin of Triplet loss, however, the model still fails to work effectively. The possible reason is that the model is too complex to enhance speech with the small-scale dataset - the complex physical SE dataset (0.6 hours) compared with theirs (about 11 hours), especially the architecture of the discriminator. Furthermore, compared with their original result (STOI 0.80 and PESQ 3.01), the USPEECH can still achieve a 0.05 higher gain in STOI and the same value of PESQ even training and evaluation in such a small-scale dataset (0.6 hours), indicating the effectiveness and efficiency of the proposed enhancement network. In addition,



compared with PHASEN [99], USPEECH w/ phy. achieves a 0.08 higher in PESQ and the equal value of STOI, indicating the proposed enhancement network outperforms in intelligibility. Besides, USPEECH w/ phy. drop more of LSD compared with only -3.4% of PHASEN, meaning that the enhancement network of USPEECH performs remarkable not only the improvement of intelligibility but also the quality of spectrograms.

When comparing the enhancement network of USPEECH trained with synthetic data (USPEECH w/ syn.) to USPEECH trained with physical data (USPEECH w/ phy.), we find that the enhancement network trained on the synthetic SE dataset achieves performance comparable to that of the system trained on physical data. Specifically, USPEECH w/ syn. achieves a PESQ score of 3.01, an STOI score of 0.85, and an LSD of 0.83. These results closely match those of USPEECH w/ phy., which achieves a PESQ of 2.90, an STOI of 0.85, and an LSD of 0.85. The similarity in PESQ and STOI scores suggests that the synthetic ultrasound spectrograms are effective for speech enhancement tasks, while the close LSD values indicate the high quality in the frequency domain of the synthetic spectrograms. Overall, these observations demonstrate that our ultrasound synthesis framework is capable of generating high-quality ultrasound spectrograms that are nearly as effective for speech enhancement as those derived from the physical dataset, confirming the robustness and practicality of using synthetic data.

### 7.1.3 Qualitative Evaluation

In addition to the quantitative evaluation, we perform a qualitative evaluation using the MOS to assess the perceptual quality of the enhanced speech from a listener’s perspective. As shown in Tab. 1, USPEECH w/ phy. achieves a MOS of 4.43, significantly outperforming the baselines such as Ultraspeech (2.13), UltraSE (2.80), and PHASEN (3.78). The results indicate that listeners perceive the speech enhanced by USPEECH w/ phy. as much clearer and more intelligible compared to other methods. The superiority of USPEECH w/ phy. in terms of MOS, along with the quantitative gains in PESQ, STOI, and LSD, demonstrates that the proposed enhancement network delivers a noticeably higher perceptual quality of recovered speech than the other baselines. Comparing USPEECH w/ syn. and phy., we observe that USPEECH w/ syn. achieves a comparable MOS of 4.45, closely matching the perceptual quality of USPEECH w/ phy. (4.43). This close result between the synthetic and physical SE datasets supports the effectiveness of the synthesis framework. It shows that the synthesis model that can generate the ultrasound spectrograms is nearly indistinguishable from the generated using physical data, proving the robustness and practicality of our synthetic data generation approach.

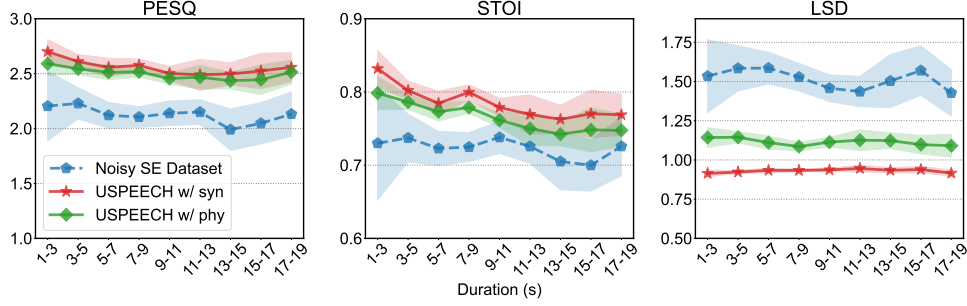
Table 2: Evaluation results on the effectiveness of USPEECH synthetic large-scale datasets.

| Dataset             | PESQ $\uparrow$ | $\Delta$ PESQ $\uparrow$ | STOI $\uparrow$ | $\Delta$ STOI $\uparrow$ | LSD $\downarrow$ | $\Delta$ LSD $\downarrow$ |
|---------------------|-----------------|--------------------------|-----------------|--------------------------|------------------|---------------------------|
| Noisy LJSpeech [41] | 1.83            | -                        | 0.78            | -                        | 1.67             | -                         |
| USPEECH             | 3.10            | +69.40%                  | 0.91            | +16.67%                  | 0.86             | -48.50%                   |
| Noisy TIMIT [30]    | 2.01            | -                        | 0.77            | -                        | 1.32             | -                         |
| USPEECH             | 2.99            | +48.76%                  | 0.89            | +15.58%                  | 0.85             | -35.61%                   |
| Noisy VCTK [96]     | 1.90            | -                        | 0.69            | -                        | 2.03             | -                         |
| USPEECH             | 2.78            | +46.32%                  | 0.83            | +20.29%                  | 0.87             | -57.14%                   |

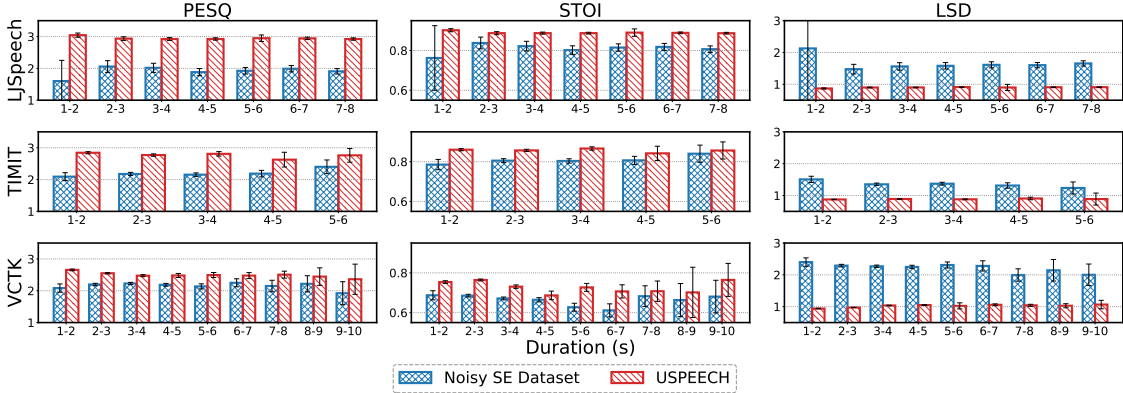
## 7.2 Ultrasonic Large-scale Datasets Synthesis

To further evaluate the effectiveness of the synthesis framework and generalizability of the enhancement network, in this experiment, we employ three large-scale synthetic SE datasets for evaluation, which are constructed using distinctive, public large-scale speech-only datasets, *i.e.*, LJSpeech [41], TIMIT [30] and VCTK [96].

As shown in Tab. 2, USPEECH consistently achieves notable gains across all metrics on the large-scale datasets, demonstrating the capability of the synthesis model to generate effective ultrasound spectrograms, even when applied to large-scale speech-only datasets. In comparison to the synthetic SE dataset (0.6 hours), the enhancement results on all large-scale datasets show superior performance across three metrics, indicating



(a) Temporal variability of physical SE dataset and synthesis SE dataset performance.



(b) Temporal variability of large-scale synthetic SE datasets performance.

Figure 8: Performance on temporal variability.

that the enhancement network of USPEECH generalizes well and benefits significantly from increased dataset scale, further supporting the robustness of the synthetic framework. When evaluating the LJSpeech [41] dataset, despite the lack of speaker diversity, the enhancement network still achieves a substantial 69.4% improvement in PESQ and a 0.06 increase in STOI, showing that the enhancement model can generalize well even when speaker variability is limited, as long as sufficient training data is provided. In contrast, for the TIMIT [30] dataset, despite the limited scale for each speaker (approximate 30-second speech for each speaker), the enhancement network still shows strong improvements, with a 48.76% increase in PESQ, a 15.58% increase in STOI, and a -35.61% drop in LSD, pointing the generalizability of the enhancement network when trained on synthetic spectrograms from a high-speaker-diversity dataset and highlighting the effectiveness of both synthesis framework as well. For the VCTK [96] dataset, the enhancement network delivers well-rounded performance across three metrics, achieving a 46.32% increase in PESQ, a 20.29% increase in STOI, along with a -57.1% drop in LSD, addressing the enhancement network perform well in both intelligibility and speech quality even with a large, diverse dataset.

Overall, the evaluation across large-scale datasets demonstrates the effectiveness of our synthetic framework and the strong generalizability of the enhancement network. The synthesis model consistently generates high-quality ultrasound spectrograms, enabling the enhancement network to perform well across varying dataset scales and speaker diversity. These results confirm that the synthetic framework is effective, making the enhancement network generalized enough to handle diverse large-scale speech enhancement tasks.

### 7.3 Temporal Variability Performance

To demonstrate the adaptability and robustness of USPEECH in handling variable-length input, we conduct experiments across multiple time intervals to evaluate the system’s resilience to temporal variations, as shown in Fig. 8. These experiments are performed on the physical SE dataset, synthetic SE dataset, and large-scale synthetic SE datasets (LJSpeech, TIMIT, and VCTK). In contrast to prior experiments that used fixed-length audio segments, this experiment introduces variability in input duration, simulating real-world

conditions where audio length fluctuates dynamically.

The results across both the physical SE dataset, synthetic SE dataset, and the ultrasonic large-scale datasets consistently show that USPEECH maintains strong and stable performance across varying input lengths in all three metrics. For the physical SE dataset, USPEECH w/ phy. achieves consistent PESQ values around 2.6-3.0, indicating the USPEECH handles longer audio inputs without significant degradation in perceptual quality. Similarly, STOI values remain robust, staying close to 0.85 across all durations, while LSD remains low, demonstrating that the system retains good spectral accuracy regardless of the input length. Besides, USPEECH trained on synthetic SE dataset (USPEECH w/ syn.) gains the close and comparable performance with USPEECH w/ phy., indicating the synthetic ultrasound spectrograms are also stable with the temporal variation. For the large-scale synthetic SE datasets, USPEECH also shows strong performance. For example, in the LJSpeech dataset, the PESQ scores for different durations range from 2.9 to 3.1, showing minimal fluctuation. Similarly, STOI scores remain above 0.85 across all temporal intervals, while LSD consistently stays below 1.0, showing the system’s capability to manage both short and long audio durations without degrading quality or intelligibility. The TIMIT and VCTK datasets display similar trends, with PESQ and STOI remaining stable across varying time intervals, and LSD values showing only slight variations, all within acceptable ranges.

Overall, the results show that USPEECH is robust and adaptable to variable-length input, maintaining stable performance across quality and intelligibility on both the collected SE and ultrasonic large-scale datasets. The system effectively handles varying audio durations without significant loss in quality or intelligibility, confirming its scalability and suitability in practical scenarios.

## 7.4 Dataset Scale Evaluation

To better understand the relationship between performance and dataset scale in both the ultrasound synthesis framework and speech enhancement network of USPEECH, we conducted comprehensive evaluations. For the synthesis framework, we incrementally vary the size of the ultrasound synthesis dataset (2.4 hours) from 25% to 100% of the full dataset, to train the synthesis model. Then, in each trial, we use the trained synthesis model to generate the synthetic SE dataset following the process in §6.2.3 and then utilize the synthetic SE dataset to train and evaluate the enhancement network. Conversely, for the enhancement network, we keep the ultrasound synthesis dataset at full scale, vary the size of the synthetic and physical SE datasets (0.6 hours) in the same rule, and utilize them to train and evaluate the enhancement network, respectively.

Tab. 3 demonstrates the results in different settings of dataset scale. Intuitively, the metrics get better as the dataset scales up. The synthesis dataset has a positive gain after the scale larger than 75%, achieving higher performance than UltraSE with the full dataset. Similarly, Tab. 4 showcases the performance of the enhancement network with both synthetic and physical datasets. The synthetic enhancement datasets with a 75% scale achieve comparable performance to the full physical enhancement dataset, confirming the system’s proficiency in generating effective synthetic ultrasound data.

Table 3: Evaluation of synthesis framework *v.s.* ultrasound synthesis dataset scale (● = 2.40h).

| Dataset                            | Scale              | PESQ ↑      | ΔPESQ ↑       | STOI ↑      | ΔSTOI ↑       | LSD ↓       | ΔLSD ↓        |
|------------------------------------|--------------------|-------------|---------------|-------------|---------------|-------------|---------------|
| Noisy SE Dataset                   | -                  | 2.33        | -             | 0.77        | -             | 1.16        | -             |
| Ultrasound<br>Synthesis<br>Dataset | ○ <sub>0.60h</sub> | 1.46        | -37.3%        | 0.60        | -22.1%        | 1.42        | +22.4%        |
|                                    | ● <sub>1.20h</sub> | 1.87        | -19.7%        | 0.65        | -15.6%        | 1.15        | -0.9%         |
|                                    | ● <sub>1.80h</sub> | 2.34        | +0.4%         | 0.78        | +1.3%         | 0.93        | -19.8%        |
|                                    | ● <sub>2.40h</sub> | <b>3.01</b> | <b>+29.2%</b> | <b>0.85</b> | <b>+10.4%</b> | <b>0.83</b> | <b>-28.4%</b> |

## 7.5 Different Noise Interference

Besides the Nonspeech [70] dataset (human non-speech dataset), we also evaluate the speech enhancement network on different datasets **without any training**, including **environmental interference**, **competing speakers interference**, and **human voice interference**, to test the robustness and adaptability to different

Table 4: Evaluation of enhancement network *v.s.* synthetic and physical SE dataset scale ( $\bullet = 0.60h$ ).

| Dataset              | Scale             | PESQ $\uparrow$ | $\Delta$ PESQ $\uparrow$ | STOI $\uparrow$ | $\Delta$ STOI $\uparrow$ | LSD $\downarrow$ | $\Delta$ LSD $\downarrow$ |
|----------------------|-------------------|-----------------|--------------------------|-----------------|--------------------------|------------------|---------------------------|
| Noisy SE Dataset     | -                 | 2.33            | -                        | 0.77            | -                        | 1.16             | -                         |
| Synthetic SE Dataset | $\bullet_{0.15h}$ | 1.72            | -26.2%                   | 0.64            | -16.9%                   | 1.22             | -5.2%                     |
|                      | $\bullet_{0.30h}$ | 1.84            | -21.0%                   | 0.71            | -7.8%                    | 1.07             | -7.8%                     |
|                      | $\bullet_{0.45h}$ | 2.72            | +16.7%                   | 0.82            | +6.5%                    | 0.85             | -26.7%                    |
|                      | $\bullet_{0.60h}$ | <b>3.01</b>     | <b>+29.2%</b>            | <b>0.85</b>     | <b>+10.4%</b>            | <b>0.83</b>      | <b>-28.4%</b>             |
| Physical SE Dataset  | $\bullet_{0.15h}$ | 1.58            | -32.2%                   | 0.63            | -18.2%                   | 1.25             | +7.8%                     |
|                      | $\bullet_{0.30h}$ | 1.80            | -22.7%                   | 0.67            | -13.0%                   | 1.10             | -5.2%                     |
|                      | $\bullet_{0.45h}$ | 2.23            | -4.3%                    | 0.75            | -2.6%                    | 0.95             | -18.2%                    |
|                      | $\bullet_{0.60h}$ | <b>2.90</b>     | <b>+24.5%</b>            | <b>0.84</b>     | <b>+9.1%</b>             | <b>0.85</b>      | <b>-26.7%</b>             |

noise distribution without training. We utilize the environmental noise dataset ESC-50 [66], consisting of animals, natural soundscapes, *etc.*. We mix it with the original dataset following the same processing with Nonspeech [70]. In competing speakers experiments, we mix each user’s dataset with others with specific SNRs randomly chosen from  $\{0, 5, 10, 15\}$  dB. For human voice interference, we collect the dataset from three other users that do not include the original dataset, then follow the process of competing speakers experiments. The results can be seen in Tab. 5.

Firstly, in the environmental interference experiments, USPEECH demonstrates impressive robustness. Without any specific training on this type of noise, USPEECH w/ syn. achieves a 32.30% gain in PESQ, a 9.09% improvement in STOI, and a 35.71% drop in LSD, matching the performance on the default human non-speech noise dataset. This suggests that USPEECH can generalize well to unseen ambient noises, highlighting the USPEECH’s ability to perform without needing targeted training. Secondly, competing speakers represent one of the most challenging scenarios in speech enhancement, where multiple speakers overlap, making it difficult to isolate and enhance one speaker’s voice. Despite this complexity, USPEECH w/ syn. achieves notable positive gains across all metrics, including a 9.59% improvement in STOI and a 7.69% reduction in LSD. Although the system’s performance here is more modest compared to environmental interference, the positive results indicate the potential for even better performance if trained specifically for this scenario. Thirdly, when testing with human voice interference, USPEECH w/ syn. again shows strong results, achieving a 14.16% gain in PESQ and an 11.43% improvement in STOI with synthetic data even without training, suggesting that ultrasound data provides additional information to help distinguish between the main speaker and interfering voices. This demonstrates that USPEECH is not only capable of enhancing speech but can also leverage ultrasound to separate different voice sources, even when not explicitly trained. In addition, USPEECH trained on synthetic SE dataset performs closely with the physical SE dataset, demonstrating the synthetic framework’s effectiveness.

Overall, the evaluation across various noise interference scenarios highlights USPEECH’s robustness and ability to generalize without additional training.

## 7.6 Unseen User Performance

To evaluate the generalizability of unseen users, we assess the USPEECH by testing it on a separate dataset gathered from unseen users. We recruit three new volunteers (two males, referred to as Male A and Male B, and one female), following the same data collection procedure. The data is collected following the same procedure. Ultrasound spectrograms are generated using the *frozen* audio-ultrasound network and pair with the corresponding audio Mel spectrograms. The dataset is then evaluated directly, without additional training, as shown in Fig. 9. The results demonstrate strong generalization across all unseen users, with USPEECH consistently outperforming the noisy dataset across all metrics. For PESQ, USPEECH scores 3.01, 2.84, and 3.10 for Male A, Male B, and the female user, respectively, compared to 2.40, 2.04, and 2.19 in the noisy dataset. In STOI, USPEECH improves by 0.06–0.09, achieving 0.86 and 0.88. The LSD results also show a reduction in spectral distortion, with values of 0.80, 0.84, and 0.79, significantly lower than the noisy dataset’s 1.11–1.18. Additionally, the overall performance on the unseen user dataset, with a PESQ

Table 5: Effectiveness of USPEECH performance in different noise interference including environmental interference, competing speakers interference, and human voice interference. The noisy datasets will be shown in different colors.

| Noise Interference                | PESQ $\uparrow$ | $\Delta$ PESQ $\uparrow$ | STOI $\uparrow$ | $\Delta$ STOI $\uparrow$ | LSD $\downarrow$ | $\Delta$ LSD $\downarrow$ |
|-----------------------------------|-----------------|--------------------------|-----------------|--------------------------|------------------|---------------------------|
| <b>Default (Human Non-speech)</b> | 2.33            | -                        | 0.77            | -                        | 1.16             | -                         |
| USPEECH w/ syn.                   | 3.01            | +29.18%                  | 0.85            | +10.39%                  | 0.83             | -28.45%                   |
| USPEECH w/ phy.                   | 2.90            | +24.46%                  | 0.84            | +9.09%                   | 0.85             | -26.72%                   |
| <b>Environmental</b>              | 2.26            | -                        | 0.77            | -                        | 1.26             | -                         |
| USPEECH w/ syn.                   | 2.99            | +32.30%                  | 0.84            | +9.09%                   | 0.81             | -35.71%                   |
| USPEECH w/ phy.                   | 2.90            | +28.32%                  | 0.83            | +7.79%                   | 0.83             | -34.13%                   |
| <b>Competing Speakers</b>         | 2.48            | -                        | 0.73            | -                        | 0.91             | -                         |
| USPEECH w/ syn.                   | 2.70            | +8.87%                   | 0.80            | +9.59%                   | 0.84             | -7.69%                    |
| USPEECH w/ phy.                   | 2.67            | +7.66%                   | 0.75            | +2.74%                   | 0.86             | -5.49%                    |
| <b>Human Voice</b>                | 2.26            | -                        | 0.70            | -                        | 1.01             | -                         |
| USPEECH w/ syn.                   | 2.58            | +14.16%                  | 0.78            | +11.43%                  | 0.86             | -14.85%                   |
| USPEECH w/ phy.                   | 2.39            | +5.75%                   | 0.76            | +8.57%                   | 0.89             | -11.88%                   |

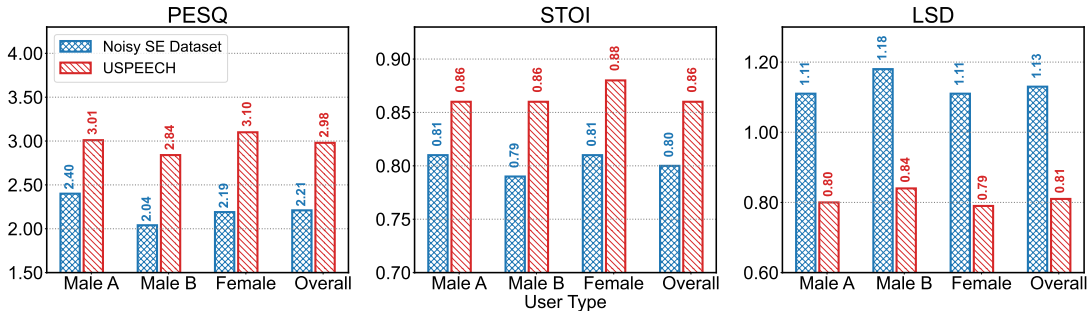


Figure 9: Performance on unseen users.

of 2.98, an STOI of 0.86, and an LSD of 0.81, closely matches the results from the seen user scenario, which achieved a PESQ of 3.01, an STOI of 0.85, and an LSD of 0.83 shown in Tab. 1. Overall, performance across all unseen users demonstrates that USPEECH generalizes effectively, maintaining high-quality speech enhancement without requiring additional training.

## 7.7 Ablation Studies

We perform the ablation studies to validate the effectiveness of the proposed components in USPEECH. The corresponding results are shown in Tab. 6.

- **w/o video pre-training** refers to skipping the contrastive video-audio pre-training phase described in §5.1.1 and directly training the synthesis model without incorporating the physical correspondence between video and ultrasound articulatory gestures. Without this pre-training, the synthesis framework witnesses a significant drop in performance. PESQ falls by 0.85 from 3.01 to 2.16, and STOI decreases by 0.12. Additionally, LSD increases by 0.16 from 0.83 to 0.99. The results show the necessity of video pre-training and the critical role of physical correspondence between video and ultrasound in generating high-quality synthetic ultrasound data.
- **w/o ultrasound branch** refers to removing the ultrasound feature concatenation before the Transformer by replacing it with a replicated speech feature in the enhancement network in §5.2.1. The system trained on the physical SE dataset suffers a notable performance decline. Although LSD re-



Table 6: Ablation study on video per-training and ultrasound branch.

| Dataset                | PESQ $\uparrow$ | $\Delta$ PESQ $\uparrow$ | STOI $\uparrow$ | $\Delta$ STOI $\uparrow$ | LSD $\downarrow$ | $\Delta$ LSD $\downarrow$ |
|------------------------|-----------------|--------------------------|-----------------|--------------------------|------------------|---------------------------|
| Noisy SE Dataset       | 2.33            | -                        | 0.77            | -                        | 1.16             | -                         |
| USPEECH w/ syn.        | 3.01            | +29.2%                   | 0.85            | +10.4%                   | 0.83             | -28.4%                    |
| w/o video pre-training | 2.16            | -7.3%                    | 0.73            | -5.2%                    | 0.99             | -14.7%                    |
| USPEECH w/ phy.        | 2.90            | +24.5%                   | 0.84            | +9.1%                    | 0.85             | -26.7%                    |
| w/o ultrasound branch  | 2.23            | -4.3%                    | 0.79            | +2.6%                    | 0.84             | -27.6%                    |

mains almost unchanged, PESQ drops by 0.67 from 2.90 to 2.23, and STOI decreases by 0.05, clearly showing the importance of integrating the ultrasound branch, which adds essential articulatory information that enhances speech intelligibility and quality.

## 7.8 Impact of Different Factors

To assess the robustness of our system under various conditions, we conduct a series of experiments, each isolating one factor among the distance from the microphone, elevation, azimuth, type of device, face mask, *etc.*, while keeping all other variables constant, as detailed in §6.1. One volunteer reads the material<sup>2</sup> under these varying conditions. For each experiment, USPEECH is evaluated using pairs of synthetic and actual ultrasound Doppler spectrograms alongside the corresponding speech Mel spectrograms. It is crucial to note that all data collected are used exclusively for testing purposes; no model training is involved. This approach ensures that the results reflect the system’s ability to perform effectively with previously unseen data.

### 7.8.1 Device Distance

The baseline configuration for our device (microphone) places it 5 cm from the mouth. In a controlled experiment, we have a volunteer reiterate the test passages at increased distances, specifically, 10, 15, and 20 cm, while keeping all other variables constant. Subsequently, we introduce a variable amount of noise to the recordings, corresponding to SNRs of  $\pm 5$  dB and 0 dB, and process the augmented data set through USPEECH, which utilizes both synthesized and actual ultrasound Doppler spectrograms. The outcomes, as depicted in Fig. 10, indicate a marginal decrement in performance as the distance between the mouth and the microphone grows. Nevertheless, the synthesis framework is capable of generating high-quality Doppler shift spectrograms, demonstrating only a slight difference in performance.

### 7.8.2 Azimuth of Device

Subsequently, we examine the effects of varying the azimuth orientation of the device while maintaining a consistent 5 cm distance from the mouth to the midpoint of the device’s bottom edge, as per the default setup, with no alteration to the elevation. We rotate the device to specific azimuthal angles relative to the mouth, namely 15, 30, and 45 degrees. Each testing dataset is mixed with the noise at randomly chosen SNRs of  $\pm 5$  and 0 dB. The results, depicted in Fig. 11, illustrate the system’s performance across these different azimuths. Despite moderate discrepancies compared to the unrotated baseline, USPEECH demonstrates a degree of enhancement, proving its robustness across different azimuth settings.

### 7.8.3 Elevation of Device

We carry out additional experiments to ascertain the resilience of the system across various microphone elevation angles. Adhering to the previously described experimental protocol, we exclusively varied the elevation of the devices to  $\pm 15$  and  $\pm 30$  degrees. Here, a negative elevation implies that the microphone is oriented more toward the speaker’s face, whereas a positive elevation indicates an orientation toward the

<sup>2</sup><https://www.bbc.com/news/technology-67379533>

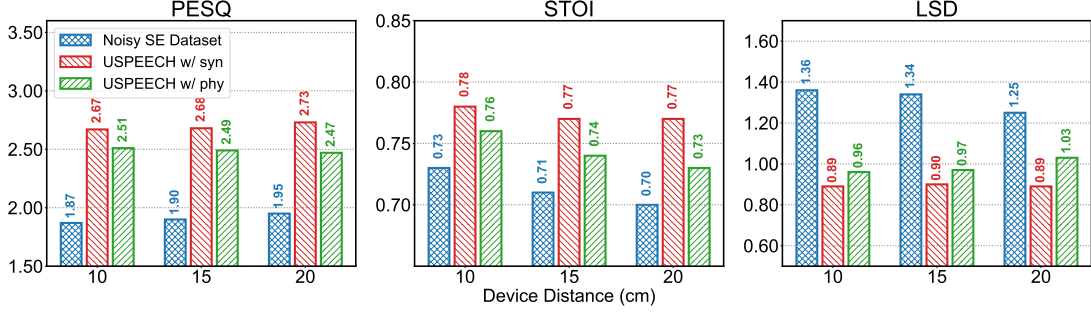


Figure 10: Performance on device distance.

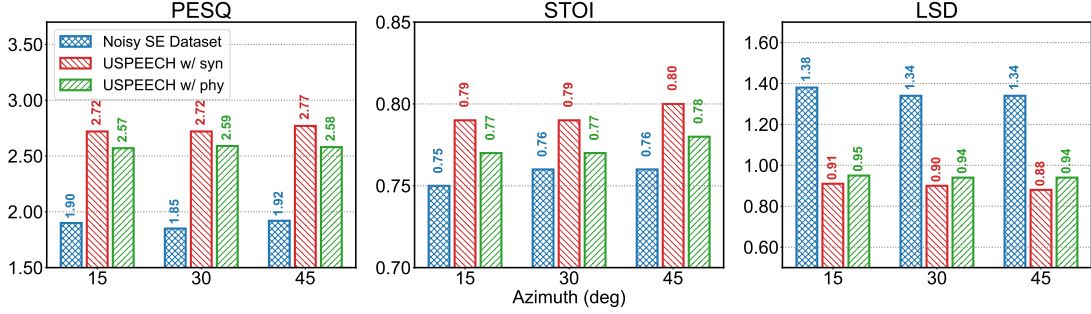


Figure 11: Performance on azimuth of device.

throat. Fig. 12 presents the outcomes of these experiments. It is evident that while there is a modest decline in performance relative to the baseline of 0 degrees, the system maintains commendable operational efficacy even at an elevation of 30 degrees.

#### 7.8.4 Type of Device

We also consider the different types of devices (*i.e.*, three models of devices: Redmi Note 5, Honor AL00T, and Lenovo PB3-690N). We can see from the Fig. 13 that the performance of USPEECH will decrease through the different types of devices due to the various layouts of microphone and loudspeaker, while the result exhibits that USPEECH can be generalized on different types of phones.

#### 7.8.5 Face Mask

Table 7: The effectiveness of face mask (● = True, ○ = False).

|                  | Mask | Synthetic | Physical | PESQ ↑ | STOI ↑ | LSD ↓ |
|------------------|------|-----------|----------|--------|--------|-------|
| Noisy SE Dataset | ●    | ✗         | ✗        | 2.22   | 0.78   | 1.29  |
|                  | ○    | ✗         | ✗        | 2.10   | 0.78   | 1.23  |
| USPEECH          | ●    | ●         | ○        | 2.90   | 0.86   | 0.85  |
|                  | ●    | ○         | ●        | 2.72   | 0.84   | 0.92  |
|                  | ○    | ●         | ○        | 2.86   | 0.86   | 0.87  |
|                  | ○    | ○         | ●        | 2.72   | 0.84   | 0.92  |

We further investigate the effect of wearing a facial mask on the speaker’s voice. By integrating noise into the collected dataset at varying SNRs of  $\pm 5$  and 0 dB, we examine the impact on the system’s performance. Tab. 7 indicates that the presence of a face mask results in a minor reduction in the PESQ and LSD.

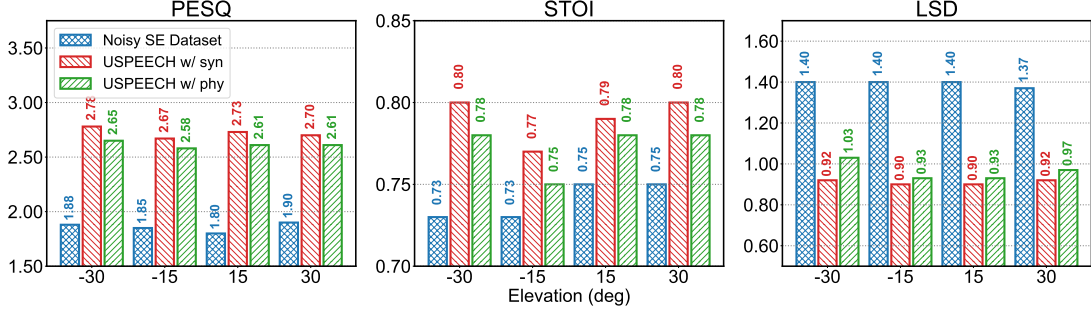


Figure 12: Performance on elevation of device.

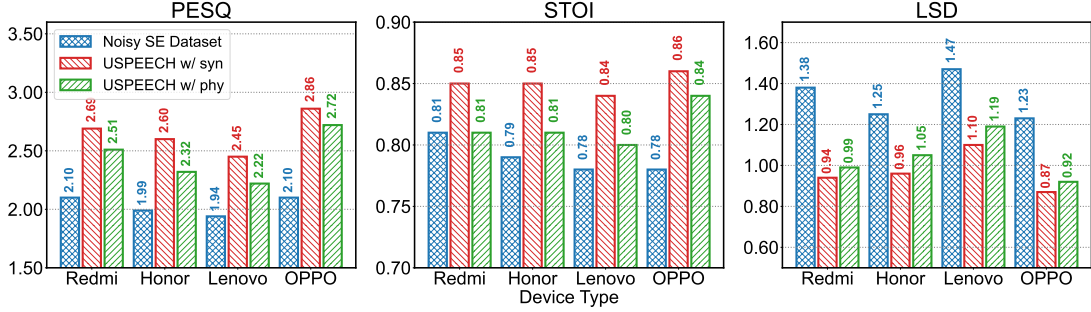


Figure 13: Performance on type of device.

However, the impact on the system, particularly regarding the STOI measure, is negligible, confirming the ultrasound system’s robustness even when the speaker is wearing the mask.

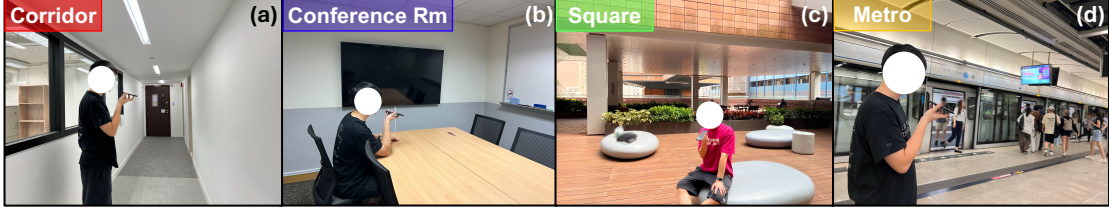
### 7.8.6 Environments

We evaluate the effect of different environments, including the corridor, conference room, square, and metro, as demonstrated in Fig. 14a. We process the data with the same diagram of the system, then directly evaluate the performance on environments. The results shown in Fig. 14b demonstrate slight degradation compared with the defaults due to no training but evaluation only and the input clean speech mixed with the ambient noise (like metro). However, all environments are still positive even without training, proving the enhancement network can be generalized to different scenarios.

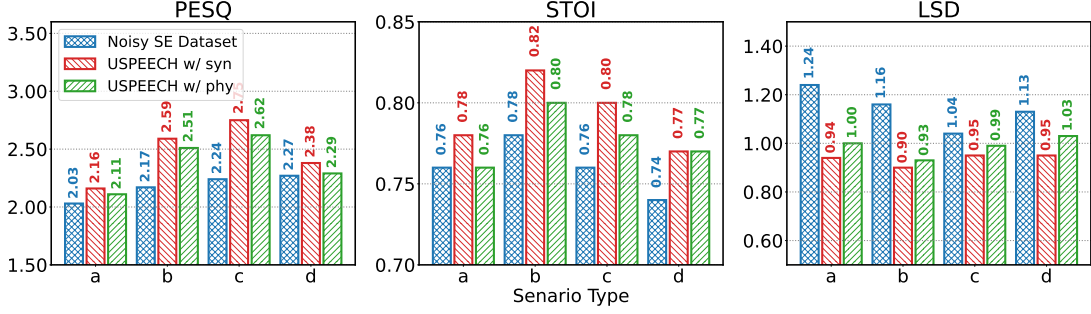
## 8 Discussion and Future Work

### 8.1 Human Effort

Collecting clean audio-ultrasound datasets is challenging due to environmental noise and ethical concerns. As mentioned above, audio can be disrupted by ambient sounds like footsteps or door movements, while ultrasound is sensitive to minor human actions like swallowing or head movements. The interference can overwhelm the desired signals, making it hard to capture clean data without a controlled environment, which requires significant effort and resources. Privacy concerns also add complexity, as many speech datasets cannot be publicly shared due to legal and ethical restrictions on personal data. To address these issues, USPEECH minimizes the need for large-scale manual data collection by first gathering a small dataset to train a synthesis model. This model then synthesizes the larger clean ultrasound-audio datasets from publicly available sources, including LJSpeech [41], TIMIT [30], and VCTK [96]. The USPEECH reduces both human effort and interference while preventing privacy and ethical concerns tied to personal data collection.



(a) Different scenarios, including the corridor, conference room, square, and metro.



(b) Performance on environments.

Figure 14: The different scenarios and the performance on environments.

## 8.2 Potential Applications

USPEECH’s ability to synthesize reliable large-scale audio-ultrasound datasets opens up opportunities for ultrasound-based sensing applications. One promising area is silent speech interfaces, where ultrasound captures articulatory movements without audible speech, benefiting individuals with speech impairments or enabling silent communication in noise-sensitive environments. Another application is hardware-free anti-eavesdropping mechanisms. By using ultrasound frequencies, speech information can be transmitted inaudibly, reducing the risk of unauthorized listening and enhancing privacy in sensitive conversations. Gesture recognition is also a potential application, where ultrasound signals detect hand gestures or body movements, enabling natural human-computer interaction. This could be applied in virtual reality, gaming, smart home control, and assistive technologies. By facilitating the generation of large-scale datasets, USPEECH supports the training of machine learning models necessary for these applications, accelerating innovation and leading to more robust sensing systems. Future research could develop prototypes and conduct user studies to evaluate effectiveness and usability in these areas.

## 8.3 Real-World Multi-User Scenarios

In our experimental evaluation (§7.5), we simulated multi-user scenarios such as competing speaker interference and human voice interference. However, we did not collect datasets from actual multi-user environments. Despite this, USPEECH still enhances noisy speech signals effectively. For future work, collecting multi-user datasets and incorporating them into the training stage could lead to better performance in real-world applications. This involves challenges like overlapping speech and dynamic acoustic environments. Incorporating real-world data could enhance the system’s ability to isolate and enhance target speech in complex settings. While the paper focuses on synthesizing large-scale audio-ultrasound datasets from small-scale datasets, addressing real-world multi-user speech separation remains an open issue for future research. Future work could explore advanced signal separation and enhancement algorithms tailored to multi-user environments, such as multi-microphone array processing and deep learning-based speech separation techniques.

## 9 Related Works

In this section, we first introduce the related works about sensing data synthesis, then we review speech enhancement with different modalities as inputs.

### 9.1 Sensing Data Synthesis

As the size of neural networks increases, so does the need for training data. Data synthesis is one way to alleviate the dilemma. Prior works proposed to synthesize data for human pose [85], IMU [46], and depth images [67] from videos and motion capture (MoCap), which are readily available as open-source data. This idea also applies to wireless data synthesis. In the early stage, researchers simulated human micro-Doppler signatures from kinematic modeling [6, 34] and MoCap datasets [20, 43, 74] to extend datasets. To generalize data collection scenarios and simplify MoCap sensor, a Kinect-based radar data simulator is proposed to generate synthetic micro-Doppler signatures [21, 75]. However, the scale of the dataset for radar data generation is much smaller than other open-sourced data. This motivated researchers to use existing large-scale IMU or video datasets to synthesize RF signals (i.e., Wi-Fi, LoRa, and mmWave) [98] and Doppler signals [2]. To the best of our knowledge, there exists no prior work on synthesizing ultrasound data for speech.

### 9.2 Speech Enhancement

#### 9.2.1 Audio-only Speech Enhancement

Considering humans can isolate the target speaker from noisy environments, extensive works dive into the task of speech enhancement. In the early stage, traditional signal preprocessing techniques, including MMSE estimation [17], spectral subtraction [42], and Kalman filtering [28], are employed to suppress the noise. With the development of deep learning, neural networks have shown remarkable performance in speech enhancement. These methods fall into either the category of time-frequency domain or time-domain. The former learn to estimate a spectrogram mask that maps the mixture input to a clean spectrogram and then generates the waveform using iSTFT [38, 57, 59, 91]. To alleviate the negative effect of inaccurate phase information, advanced methods also consider estimating the phase to facilitate clean waveform generation [19, 99]. As for the latter, time-domain methods take noisy audio waveform as the input and predict the clean waveform directly [51, 64, 65, 77]. Compared with time-frequency domain methods, time-domain methods process the sparse representation of audio signal, resulting in relatively slower convergence and lower performance.

#### 9.2.2 Multimodal Speech Enhancement

To improve the performance of speech enhancement, various modalities that can provide complementary information are explored, such as vision, accelerometer, mmWave radar, ultrasound, *etc.*. Extensive methods leverage the correspondence between audio and visual cues in video for speech enhancement, as the speaker’s facial information has been shown to improve human listening. These approaches rely on lip movement [1, 27, 61] and facial frames [11, 29] to separate or suppress sounds that do not correspond to the speaker in the video. Beyond this, the bone-conductance accelerometer mounted in an earbud captures the local vibration induced by the speaker, and this fact leads to many studies on speech enhancement utilizing accelerometer-audio information. For example, [89] and [82] explored the deep learning network incorporating audio and accelerometer, while VibVoice [35] focused on speech enhancement with real-world noise. Similarly, mmWave radar detects vibrations of the human throat and movements of lip motion in a non-contact manner to provide auxiliary information, enhancing speech features. The uniqueness of the mmWave signal has contributed to various speech-related tasks, including speech recognition [23, 103], speaker recognition [48], and speech enhancement and separation [62]. However, cameras easily leak private and sensitive information, and they require good lighting conditions. Besides cameras, accelerometers and mmWave radar are additionally installed or employed sensors, limiting their ubiquity in practice.



### 9.2.3 Ultrasound-based Speech Enhancement

In contrast to the above modalities, ultrasound is derived from the loudspeaker that is common in commodity mobile phones and headphones and does not suffer from light and privacy issues. Thus, recent works exploit ultrasound to capture lip movement for guiding speech enhancement. UltraSE [78] fused noisy speech and ultrasound to separate the speaker’s voice from noise. WaveVoice [101] proposed a lightweight network to implement ultrasound-based speech enhancement. UltraSpeech [14] designed a complex-valued network that combines speech and ultrasound in the feature domain for speech enhancement. In addition to using speakers in mobile phones, EarSE [16] modified the COTS headphones to establish an acoustic sensing field from the ear pad to the boom microphone for speech enhancement using ultrasound and speech. However, most existing methods are suffering in collecting training data, which is labor-intensive and time-consuming. Besides, the setups are also constrained which leads to less diversity and generalization. In contrast, USPEECH pioneers the first step to utilize the large-scale video-audio dataset to synthesize the ultrasound spectrogram, minimizing the human effort in data collection, while boosting the performance by training on vary large-scale synthetic datasets.

## 10 Conclusions

In this paper, we introduce USPEECH, the first ultrasound spectrogram synthesis framework for ultrasound-based speech enhancement with minimal human effort. USPEECH leverages audio as the bridge to connect modalities of video and ultrasound for ultrasound synthesis. On this basis, USPEECH presents an effective network for speech enhancement using synthetic ultrasound data. The proposed USPEECH reduces human efforts for data collection and processing and promises improved speech quality and intelligibility. Our comprehensive evaluation experiments show the remarkable performance of USPEECH, achieving comparable results between synthetic and physical data and outperforming state-of-the-art ultrasound-based speech enhancement baselines. Moreover, USPEECH has the possibility to boost the speech enhancement performance on noisy large-scale speech-only datasets by leveraging the ultrasound data generated from them.

## References

- [1] Triantafyllos Afouras, Joon Son Chung, and Andrew Zisserman. The conversation: Deep audio-visual speech enhancement. *arXiv preprint arXiv:1804.04121*, 2018.
- [2] Karan Ahuja, Yue Jiang, Mayank Goel, and Chris Harrison. Vid2doppler: Synthesizing doppler radar data from videos for training privacy-preserving activity recognition. In *Proceedings of the 2021 CHI Conference on Human Factors in Computing Systems*, pages 1–10, 2021.
- [3] Jont B Allen. How do humans process and recognize speech? *IEEE Transactions on speech and audio processing*, 2(4):567–577, 1994.
- [4] Yang Bai, Li Lu, Jerry Cheng, Jian Liu, Yingying Chen, and Jiadi Yu. Acoustic-based sensing and applications: A survey. *Computer Networks*, 181:107447, 2020. ISSN 1389-1286.
- [5] Sakshi Bajpai and D Radha. Smart phone as a controlling device for smart home using speech recognition. In *2019 International Conference on Communication and Signal Processing (ICCSP)*, pages 0701–0705. IEEE, 2019.
- [6] Igal Bilik and Joseph Tabrikian. Radar target classification using doppler signatures of human locomotion models. *IEEE Transactions on Aerospace and Electronic Systems*, 43(4):1510–1522, 2007.
- [7] Crystal Boyd. Happiness is a journey, 2024. URL <https://happineessisajourney.com/>. 2024-01-27.
- [8] NM Brooke and Quentin Summerfield. Analysis, synthesis, and perception of visible articulatory movements. *Journal of phonetics*, 11(1):63–76, 1983.
- [9] Siew Wen Chin, Kah Phooi Seng, and Li-Minn Ang. Audio-visual speech processing for human computer interaction. In *Advances in robotics and virtual reality*, pages 135–165. Springer, 2012.

- [10] J. S. Chung and A. Zisserman. Lip reading in the wild. In *Asian Conference on Computer Vision*, 2016.
- [11] Soo-Whan Chung, Soyeon Choe, Joon Son Chung, and Hong-Goo Kang. Facefilter: Audio-visual speech separation using still images. *arXiv preprint arXiv:2005.07074*, 2020.
- [12] F. L. Darley, A. E. Aronson, and J. R. Brown. *Motor Speech Disorders*. W.B. Saunders Company, Philadelphia, PA, 3 edition, 1975.
- [13] Jia Deng, Wei Dong, Richard Socher, Li-Jia Li, Kai Li, and Li Fei-Fei. Imagenet: A large-scale hierarchical image database. In *2009 IEEE conference on computer vision and pattern recognition*, pages 248–255. Ieee, 2009.
- [14] Han Ding, Yizhan Wang, Hao Li, Cui Zhao, Ge Wang, Wei Xi, and Jizhong Zhao. Ultraspeech: Speech enhancement by interaction between ultrasound and speech. *Proceedings of the ACM on Interactive, Mobile, Wearable and Ubiquitous Technologies*, 6(3):1–25, 2022.
- [15] Alexey Dosovitskiy, Lucas Beyer, Alexander Kolesnikov, Dirk Weissenborn, Xiaohua Zhai, Thomas Unterthiner, Mostafa Dehghani, Matthias Minderer, Georg Heigold, Sylvain Gelly, et al. An image is worth 16x16 words: Transformers for image recognition at scale. *arXiv preprint arXiv:2010.11929*, 2020.
- [16] Di Duan, Yongliang Chen, Weitao Xu, and Tianxing Li. Earsee: Bringing robust speech enhancement to cots headphones. *Proceedings of the ACM on Interactive, Mobile, Wearable and Ubiquitous Technologies*, 7(4):1–33, 2024.
- [17] Yariv Ephraim and David Malah. Speech enhancement using a minimum-mean square error short-time spectral amplitude estimator. *IEEE Transactions on acoustics, speech, and signal processing*, 32(6):1109–1121, 1984.
- [18] Yariv Ephraim and Harry L Van Trees. A signal subspace approach for speech enhancement. *IEEE Transactions on speech and audio processing*, 3(4):251–266, 1995.
- [19] Hakan Erdogan, John R Hershey, Shinji Watanabe, and Jonathan Le Roux. Phase-sensitive and recognition-boosted speech separation using deep recurrent neural networks. In *2015 IEEE International Conference on Acoustics, Speech and Signal Processing (ICASSP)*, pages 708–712. IEEE, 2015.
- [20] Baris Erol and Sevgi Zubeyde Gurbuz. A kinect-based human micro-doppler simulator. *IEEE Aerospace and Electronic Systems Magazine*, 30(5):6–17, 2015.
- [21] Baris Erol and Sevgi Zubeyde Gurbuz. A kinect-based human micro-doppler simulator. *IEEE Aerospace and Electronic Systems Magazine*, 30(5):6–17, 2015. doi: 10.1109/MAES.2015.7119820.
- [22] Grant Fairbanks. Voice and articulation drillbook. (*No Title*), 1960.
- [23] Long Fan, Lei Xie, Xinran Lu, Yi Li, Chuyu Wang, and Sanglu Lu. mmmic: Multi-modal speech recognition based on mmwave radar. In *IEEE INFOCOM 2023-IEEE Conference on Computer Communications*, pages 1–10. IEEE, 2023.
- [24] Christoph Feichtenhofer, Haoqi Fan, Jitendra Malik, and Kaiming He. Slowfast networks for video recognition. In *Proceedings of the IEEE/CVF international conference on computer vision*, pages 6202–6211, 2019.
- [25] Jean-Yves Fourniols, Nadim Nasreddine, Christophe Escriba, Pascal Acco, Julien Roux, and Georges Soto-Romero. An overview of basics speech recognition and autonomous approach for smart home iot low power devices. *Journal of Signal and Information Processing*, 9(4):239, 2018.
- [26] Aviv Gabbay, Asaph Shamir, and Shmuel Peleg. Visual speech enhancement. *arXiv preprint arXiv:1711.08789*, 2017.

- [27] Aviv Gabbay, Asaph Shamir, and Shmuel Peleg. Visual speech enhancement. In *Proc. Interspeech 2018*, pages 1170–1174, 2018.
- [28] Sharon Gannot, David Burshtein, and Ehud Weinstein. Iterative and sequential kalman filter-based speech enhancement algorithms. *IEEE Transactions on speech and audio processing*, 6(4):373–385, 1998.
- [29] Ruohan Gao and Kristen Grauman. Visualvoice: Audio-visual speech separation with cross-modal consistency. In *2021 IEEE/CVF Conference on Computer Vision and Pattern Recognition (CVPR)*, pages 15490–15500. IEEE, 2021.
- [30] John S Garofolo. Timit acoustic phonetic continuous speech corpus. *Linguistic Data Consortium, 1993*, 1993.
- [31] Jort F Gemmeke, Daniel PW Ellis, Dylan Freedman, Aren Jansen, Wade Lawrence, R Channing Moore, Manoj Plakal, and Marvin Ritter. Audio set: An ontology and human-labeled dataset for audio events. In *2017 IEEE international conference on acoustics, speech and signal processing (ICASSP)*, pages 776–780. IEEE, 2017.
- [32] Bryan Gick, Ian Wilson, and Donald Derrick. *Articulatory phonetics*. John Wiley & Sons, 2013.
- [33] Jun Gong, Aakar Gupta, and Hrvoje Benko. Acustico: Surface tap detection and localization using wrist-based acoustic tdoa sensing. In *Proceedings of the 33rd Annual ACM Symposium on User Interface Software and Technology, UIST '20*, page 406–419, New York, NY, USA, 2020. Association for Computing Machinery. ISBN 9781450375146.
- [34] SR Groot, AG Yarovoy, RIA Harmanny, and JN Driessen. Model-based classification of human motion: Particle filtering applied to the micro-doppler spectrum. In *2012 9th European Radar Conference*, pages 198–201. IEEE, 2012.
- [35] Lixing He, Haozheng Hou, Shuyao Shi, Xian Shuai, and Zhenyu Yan. Towards bone-conducted vibration speech enhancement on head-mounted wearables. In *Proceedings of the 21st Annual International Conference on Mobile Systems, Applications and Services*, pages 14–27, 2023.
- [36] Douglas N Honorof, Jill McCullough, and Barbara Somerville. Comma gets a cure. *diagnostic passage*, 2000.
- [37] Guoning Hu and DeLiang Wang. A tandem algorithm for pitch estimation and voiced speech segregation. *IEEE Transactions on Audio, Speech, and Language Processing*, 18(8):2067–2079, 2010.
- [38] Yanxin Hu, Yun Liu, Shubo Lv, Mengtao Xing, Shimin Zhang, Yihui Fu, Jian Wu, Bihong Zhang, and Lei Xie. Dccrn: Deep complex convolution recurrent network for phase-aware speech enhancement. *arXiv preprint arXiv:2008.00264*, 2020.
- [39] Giancarlo Iannizzotto, Lucia Lo Bello, Andrea Nucita, and Giorgio Mario Grasso. A vision and speech enabled, customizable, virtual assistant for smart environments. In *2018 11th International Conference on Human System Interaction (HSI)*, pages 50–56. IEEE, 2018.
- [40] International Telecommunication Union. ITU-T Recommendation P.862.2: Wideband extension to Recommendation P.862 for the assessment of wideband telephone networks and speech codecs. <https://www.itu.int/rec/T-REC-P.862.2>, 2007. Accessed: [23 MAR 2024].
- [41] Keith Ito and Linda Johnson. The lj speech dataset. <https://keithito.com/LJ-Speech-Dataset/>, 2017.
- [42] Sunil Kamath, Philipos Loizou, et al. A multi-band spectral subtraction method for enhancing speech corrupted by colored noise. In *ICASSP*, volume 4, pages 44164–44164. Citeseer, 2002.

- [43] Cesur Karabacak, Sevgi Z Gurbuz, Ali C Gurbuz, Mehmet B Guldogan, Gustaf Hendeby, and Fredrik Gustafsson. Knowledge exploitation for human micro-doppler classification. *IEEE Geoscience and Remote Sensing Letters*, 12(10):2125–2129, 2015.
- [44] Will Kay, Joao Carreira, Karen Simonyan, Brian Zhang, Chloe Hillier, Sudheendra Vijayanarasimhan, Fabio Viola, Tim Green, Trevor Back, Paul Natsev, et al. The kinetics human action video dataset. *arXiv preprint arXiv:1705.06950*, 2017.
- [45] Qiuqiang Kong, Yin Cao, Turab Iqbal, Yuxuan Wang, Wenwu Wang, and Mark D Plumbley. Panns: Large-scale pretrained audio neural networks for audio pattern recognition. *IEEE/ACM Transactions on Audio, Speech, and Language Processing*, 28:2880–2894, 2020.
- [46] Hyeokhyen Kwon, Catherine Tong, Harish Haresamudram, Yan Gao, Gregory D. Abowd, Nicholas D. Lane, and Thomas Plötz. Imutube: Automatic extraction of virtual on-body accelerometry from video for human activity recognition. *Proc. ACM Interact. Mob. Wearable Ubiquitous Technol.*, 4(3), sep 2020.
- [47] Liyuan Liu, Haoming Jiang, Pengcheng He, Weizhu Chen, Xiaodong Liu, Jianfeng Gao, and Jiawei Han. On the variance of the adaptive learning rate and beyond. *arXiv preprint arXiv:1908.03265*, 2019.
- [48] Tiantian Liu, Feng Lin, Chao Wang, Chenhan Xu, Xiaoyu Zhang, Zhengxiong Li, Wen Yao Xu, Ming-Chun Huang, and Kui Ren. Wavoid: Robust and secure multi-modal user identification via mmwave-voice mechanism. In *Proceedings of the 36th Annual ACM Symposium on User Interface Software and Technology*, pages 1–15, 2023.
- [49] Ilya Loshchilov and Frank Hutter. Fixing weight decay regularization in adam. 2018.
- [50] Simian Luo, Chuanhao Yan, Chenxu Hu, and Hang Zhao. Diff-foley: Synchronized video-to-audio synthesis with latent diffusion models. *Advances in Neural Information Processing Systems*, 36, 2024.
- [51] Yi Luo and Nima Mesgarani. Conv-tasnet: Surpassing ideal time–frequency magnitude masking for speech separation. *IEEE/ACM transactions on audio, speech, and language processing*, 27(8):1256–1266, 2019.
- [52] Wenguang Mao, Jian He, and Lili Qiu. Cat: high-precision acoustic motion tracking. In *Proceedings of the 22nd Annual International Conference on Mobile Computing and Networking*, pages 69–81, 2016.
- [53] Antonio Martínez-Colón, Raquel Viciania-Abad, Jose Manuel Perez-Lorenzo, Christine Evers, and Patrick A Naylor. An audio enhancement system to improve intelligibility for social-awareness in hri. *Multimedia Tools and Applications*, 81(3):3327–3350, 2022.
- [54] Cosmin Munteanu, Pourang Irani, Sharon Oviatt, Matthew Aylett, Gerald Penn, Shimei Pan, Nikhil Sharma, Frank Rudzicz, Randy Gomez, Ben Cowan, et al. Designing speech, acoustic and multi-modal interactions. In *Proceedings of the 2017 CHI conference extended abstracts on human factors in computing systems*, pages 601–608, 2017.
- [55] Satoshi Nakamura, Konstantin Markov, Hiromi Nakaiwa, Gen-ichiro Kikui, Hisashi Kawai, Takatoshi Jitsuhiro, J-S Zhang, Hirofumi Yamamoto, Eiichiro Sumita, and Seiichi Yamamoto. The atr multilingual speech-to-speech translation system. *IEEE Transactions on Audio, Speech, and Language Processing*, 14(2):365–376, 2006.
- [56] Rajalakshmi Nandakumar, Vikram Iyer, Desney Tan, and Shyamnath Gollakota. Fingerio: Using active sonar for fine-grained finger tracking. In *Proceedings of the 2016 CHI Conference on Human Factors in Computing Systems*, pages 1515–1525, 2016.
- [57] Arun Narayanan and DeLiang Wang. Ideal ratio mask estimation using deep neural networks for robust speech recognition. In *2013 IEEE international conference on acoustics, speech and signal processing*, pages 7092–7096. IEEE, 2013.

- [58] Arun Narayanan and DeLiang Wang. Investigation of speech separation as a front-end for noise robust speech recognition. *IEEE/ACM Transactions on Audio, Speech, and Language Processing*, 22(4):826–835, 2014.
- [59] Aditya Arie Nugraha, Antoine Liutkus, and Emmanuel Vincent. Multichannel audio source separation with deep neural networks. *IEEE/ACM Transactions on Audio, Speech, and Language Processing*, 24(9):1652–1664, 2016.
- [60] Aaron van den Oord, Yazhe Li, and Oriol Vinyals. Representation learning with contrastive predictive coding. *arXiv preprint arXiv:1807.03748*, 2018.
- [61] Andrew Owens and Alexei A Efros. Audio-visual scene analysis with self-supervised multisensory features. In *Proceedings of the European conference on computer vision (ECCV)*, pages 631–648, 2018.
- [62] Muhammed Zahid Ozturk, Chenshu Wu, Beibei Wang, Min Wu, and KJ Ray Liu. Radio ses: mmwave-based audioradio speech enhancement and separation system. *IEEE/ACM Transactions on Audio, Speech, and Language Processing*, 31:1333–1347, 2023.
- [63] Kuldeep Paliwal, Kamil Wójcicki, and Benjamin Shannon. The importance of phase in speech enhancement. *speech communication*, 53(4):465–494, 2011.
- [64] Ashutosh Pandey and DeLiang Wang. Tcn: Temporal convolutional neural network for real-time speech enhancement in the time domain. In *ICASSP 2019-2019 IEEE International Conference on Acoustics, Speech and Signal Processing (ICASSP)*, pages 6875–6879. IEEE, 2019.
- [65] Santiago Pascual, Antonio Bonafonte, and Joan Serra. Segan: Speech enhancement generative adversarial network. *arXiv preprint arXiv:1703.09452*, 2017.
- [66] Karol J Piczak. Esc: Dataset for environmental sound classification. In *Proceedings of the 23rd ACM international conference on Multimedia*, pages 1015–1018, 2015.
- [67] Benjamin Planche, Ziyang Wu, Kai Ma, Shanhui Sun, Stefan Kluckner, Oliver Lehmann, Terrence Chen, Andreas Hutter, Sergey Zakharov, Harald Kosch, and Jan Ernst. Depthsynth: Real-time realistic synthetic data generation from cad models for 2.5d recognition. In *2017 International Conference on 3D Vision (3DV)*, pages 1–10, 2017. doi: 10.1109/3DV.2017.00011.
- [68] Lawrence R Rabiner and Biing-Hwang Juang. *Fundamentals of speech recognition*. Tsinghua University Press, 1999.
- [69] Alec Radford, Jong Wook Kim, Chris Hallacy, Aditya Ramesh, Gabriel Goh, Sandhini Agarwal, Girish Sastry, Amanda Askell, Pamela Mishkin, Jack Clark, et al. Learning transferable visual models from natural language supervision. In *International conference on machine learning*, pages 8748–8763. PMLR, 2021.
- [70] Muhammad Mamunur Rashid, Guiqing Li, and Chengrui Du. Nonspeech7k dataset: Classification and analysis of human non-speech sound. *IET Signal Processing*, 17(6):e12233, 2023.
- [71] Olaf Ronneberger, Philipp Fischer, and Thomas Brox. U-net: Convolutional networks for biomedical image segmentation. In *Medical image computing and computer-assisted intervention—MICCAI 2015: 18th international conference, Munich, Germany, October 5-9, 2015, proceedings, part III 18*, pages 234–241. Springer, 2015.
- [72] Ernst H Rothaus. Ieee recommended practice for speech quality measurements. *IEEE Transactions on Audio and Electroacoustics*, 17(3):225–246, 1969.
- [73] Seeing Speech. How uti works. <https://www.seeingspeech.ac.uk/how-uti-works/>, n.d. Accessed: 2024-03-31.



- [74] Mehmet S Seyfioglu, Baris Erol, Sevgi Z Gurbuz, and Moeness G Amin. Diversified radar micro-doppler simulations as training data for deep residual neural networks. In *2018 IEEE radar Conference (radarConf18)*, pages 0612–0617. IEEE, 2018.
- [75] Mehmet Saygin Seyfioglu, Baris Erol, Sevgi Zubeyde Gurbuz, and Moeness G. Amin. Dnn transfer learning from diversified micro-doppler for motion classification. *IEEE Transactions on Aerospace and Electronic Systems*, 55(5):2164–2180, 2019. doi: 10.1109/TAES.2018.2883847.
- [76] Maureen Stone. A guide to analysing tongue motion from ultrasound images. *Clinical linguistics & phonetics*, 19(6-7):455–501, 2005.
- [77] Cem Subakan, Mirco Ravanelli, Samuele Cornell, Mirko Bronzi, and Jianyuan Zhong. Attention is all you need in speech separation. In *ICASSP 2021-2021 IEEE International Conference on Acoustics, Speech and Signal Processing (ICASSP)*, pages 21–25. IEEE, 2021.
- [78] Ke Sun and Xinyu Zhang. Ultrase: single-channel speech enhancement using ultrasound. In *Proceedings of the 27th annual international conference on mobile computing and networking*, pages 160–173, 2021.
- [79] Ke Sun, Ting Zhao, Wei Wang, and Lei Xie. Vskin: Sensing touch gestures on surfaces of mobile devices using acoustic signals. In *Proceedings of the 24th annual international conference on mobile computing and networking*, pages 591–605, 2018.
- [80] Zhuoyi Sun, Yingdan Li, Hanjun Jiang, Fei Chen, Xiang Xie, and Zhihua Wang. A supervised speech enhancement method for smartphone-based binaural hearing aids. *IEEE Transactions on Biomedical Circuits and Systems*, 14(5):951–960, 2020.
- [81] Cees H Taal, Richard C Hendriks, Richard Heusdens, and Jesper Jensen. A short-time objective intelligibility measure for time-frequency weighted noisy speech. In *2010 IEEE international conference on acoustics, speech and signal processing*, pages 4214–4217. IEEE, 2010.
- [82] Marco Tagliasacchi, Yunpeng Li, Karolis Misiunas, and Dominik Roblek. Seanet: A multi-modal speech enhancement network. *arXiv preprint arXiv:2009.02095*, 2020.
- [83] Kristin J Teplansky, Brian Y Tsang, and Jun Wang. Tongue and lip motion patterns in voiced, whispered, and silent vowel production. In *Proc. International Congress of Phonetic Sciences*, pages 1–5, 2019.
- [84] University of Wisconsin - Dialect Research. Arthur the Rat. <https://dare.wisc.edu/audio/arthur-the-rat/>, 2023. Accessed: 2023-09-30.
- [85] Gül Varol, Javier Romero, Xavier Martin, Naureen Mahmood, Michael J. Black, Ivan Laptev, and Cordelia Schmid. Learning from synthetic humans. In *2017 IEEE Conference on Computer Vision and Pattern Recognition (CVPR)*, pages 4627–4635, 2017. doi: 10.1109/CVPR.2017.492.
- [86] Ashish Vaswani, Noam Shazeer, Niki Parmar, Jakob Uszkoreit, Llion Jones, Aidan N Gomez, Łukasz Kaiser, and Illia Polosukhin. Attention is all you need. *Advances in neural information processing systems*, 30, 2017.
- [87] Wolfgang Wahlster. *Verbmobil: foundations of speech-to-speech translation*. Springer Science & Business Media, 2013.
- [88] Yukoh Wakabayashi, Takahiro Fukumori, Masato Nakayama, Takanobu Nishiura, and Yoichi Yamashita. Single-channel speech enhancement with phase reconstruction based on phase distortion averaging. *IEEE/ACM Transactions on Audio, Speech, and Language Processing*, 26(9):1559–1569, 2018.
- [89] Heming Wang, Xueliang Zhang, and DeLiang Wang. Fusing bone-conduction and air-conduction sensors for complex-domain speech enhancement. *IEEE/ACM transactions on audio, speech, and language processing*, 30:3134–3143, 2022.

- [90] Zhou Wang, Alan C Bovik, Hamid R Sheikh, and Eero P Simoncelli. Image quality assessment: from error visibility to structural similarity. *IEEE transactions on image processing*, 13(4):600–612, 2004.
- [91] Donald S Williamson, Yuxuan Wang, and DeLiang Wang. Complex ratio masking for monaural speech separation. *IEEE/ACM transactions on audio, speech, and language processing*, 24(3):483–492, 2015.
- [92] Milo Winter. The north wind and the sun. <http://mythfolklore.net/aesopica/milowinter/141.htm>, Year of Publication. 2024-01-27.
- [93] Joe Wolfe, Maëva Garnier, Nathalie Henrich Bernardoni, and John Smith. The mechanics and acoustics of the singing voice: Registers, resonances and the source–filter interaction. In *The Routledge Companion to Interdisciplinary Studies in Singing, Volume I: Development*, pages 64–78. Routledge, 2020.
- [94] Yong Xu, Jun Du, Li-Rong Dai, and Chin-Hui Lee. An experimental study on speech enhancement based on deep neural networks. *IEEE Signal processing letters*, 21(1):65–68, 2013.
- [95] Yong Xu, Jun Du, Li-Rong Dai, and Chin-Hui Lee. A regression approach to speech enhancement based on deep neural networks. *IEEE/ACM transactions on audio, speech, and language processing*, 23(1):7–19, 2014.
- [96] Junichi Yamagishi. English multi-speaker corpus for cstr voice cloning toolkit, 2012. URL <http://homepages.inf.ed.ac.uk/jyamagis/page3/page58/page58.html>.
- [97] Ryuichi Yamamoto, Eunwoo Song, and Jae-Min Kim. Parallel wavegan: A fast waveform generation model based on generative adversarial networks with multi-resolution spectrogram. In *ICASSP 2020-2020 IEEE International Conference on Acoustics, Speech and Signal Processing (ICASSP)*, pages 6199–6203. IEEE, 2020.
- [98] Huanqi Yang, Mingda Han, Mingda Jia, Zehua Sun, Pengfei Hu, Yu Zhang, Tao Gu, , and Weitao Xu. Xgait: Cross-modal translation via deep generative sensing for rf-based gait recognition. In *Proceedings of the 21th ACM Conference on Embedded Networked Sensor Systems, SenSys ’23*, Istanbul, Turkiye, 2023. Association for Computing Machinery.
- [99] Dacheng Yin, Chong Luo, Zhiwei Xiong, and Wenjun Zeng. Phasen: A phase-and-harmonics-aware speech enhancement network. In *Proceedings of the AAAI Conference on Artificial Intelligence*, volume 34, pages 9458–9465, 2020.
- [100] Sangki Yun, Yi-Chao Chen, Huihuang Zheng, Lili Qiu, and Wenguang Mao. Strata: Fine-grained acoustic-based device-free tracking. In *Proceedings of the 15th annual international conference on mobile systems, applications, and services*, pages 15–28, 2017.
- [101] Qian Zhang, Dong Wang, Run Zhao, Yinggang Yu, and Junjie Shen. Sensing to hear: Speech enhancement for mobile devices using acoustic signals. *Proceedings of the ACM on Interactive, Mobile, Wearable and Ubiquitous Technologies*, 5(3):1–30, 2021.
- [102] Running Zhao, Jiangtao Yu, Tingle Li, Hang Zhao, and Edith C. H. Ngai. Radio2Speech: High Quality Speech Recovery from Radio Frequency Signals. In *Proc. Interspeech 2022*, pages 4666–4670, 2022. doi: 10.21437/Interspeech.2022-738.
- [103] Running Zhao, Jiangtao Yu, Hang Zhao, and Edith CH Ngai. Radio2text: Streaming speech recognition using mmwave radio signals. *Proceedings of the ACM on Interactive, Mobile, Wearable and Ubiquitous Technologies*, 7(3):1–28, 2023.

## A Reading Materials

Tab. A1 outlines the reading materials used in our study, detailing the title, reference, and type for each item. The first is the article, the following four news and the last five are the reading materials.

Table A1: Reading Materials

| Title   | Category          |
|---|-------------------|
| Happiness is a Journey [7]  | article           |
| Microsoft says Teams and Xbox fixed in UK and Europe <sup>3</sup>         | news              |
| UK economy flatlines as higher interest rates bite <sup>4</sup>           | news              |
| Elon Musk tells Rishi Sunak AI will put an end to work <sup>5</sup>       | news              |
| US and China reach 'some agreements' on climate - John Kerry <sup>6</sup> | news              |
| Voice and articulation drillbook [22]                                     | reading materials |
| Comma gets a cure [36]  | reading materials |
| The North Wind and the Sun [92]   | reading materials |
| The Story of Arthur the Rat [84]  | reading materials |
| Motor Speech Disorders [12]   | reading materials |

## B MOS Rating

Tab. B1 shows the MOS score from 1 to 5 and the corresponding description.

Table B1: MOS Rating Scale

| MOS | Quality   | Impairment                   |
|-----|-----------|------------------------------|
| 5   | Excellent | Imperceptible                |
| 4   | Good      | Perceptible but not annoying |
| 3   | Fair      | Slightly annoying            |
| 2   | Poor      | Annoying                     |
| 1   | Bad       | Very annoying                |

<sup>3</sup><https://www.bbc.com/news/technology-67379533>

<sup>4</sup><https://www.bbc.com/news/business-67370315>

<sup>5</sup><https://www.bbc.com/news/uk-67302048>

<sup>6</sup><https://www.bbc.com/news/world-asia-67376471>